

Glucose Detection Devices and Methods Based on Metal–Organic Frameworks and Related Materials

Muhammad Adeel,* Kanwal Asif, Md. Mahbubur Rahman,* Salvatore Daniele,* Vincenzo Canzonieri, and Flavio Rizzolio

Assessment of glucose concentration is important in the diagnosis and treatment of diabetes. Since the introduction of enzymatic glucose biosensors, scientific and technological advances in nanomaterials have led to the development of new generations of glucose sensors. This field has witnessed major developments over the last decade, as the novel nanomaterials are capable of efficiently catalyzing glucose directly (i.e., act as artificial enzymes, therefore defined nanozymes) or to entrap enzymes that are able to oxidize glucose. Among other nanomaterials, metal–organic frameworks (MOFs) have recently provided a tremendous basis to construct glucose sensing devices. MOFs are large porous crystalline compounds with versatile structural and tuneable chemical properties. In addition, they possess catalytic, peroxidase-like, and electrochemical redox activity. This review comprehensively summarizes the general characteristics of MOFs, their subtypes, and MOF composites, as well as MOF-derived materials employed to construct electrochemical, optical, transistor, and microfluidic devices for the detection of glucose. They include enzymatic, nonenzymatic, wearable, and flexible sensing devices and methods. The review also outlines the design and synthesis of MOFs and the working principles of the different transduction-based glucose sensors and highlights the current challenges and future perspectives.

1. Introduction

Diabetes is one of the lethal diseases that kills a large number of people around the globe each year, and it also leads to several other illnesses such as kidney failure, stroke, and blindness.^[1,2] It is one of the most diagnosed diseases having an increasing number of patients every year. For example, global diabetes cases have been projected to be 463 millions in 2019, which will raise to about 578 and 700 millions by 2030 and 2045, respectively.^[3,4] The deficiency of insulin production in the pancreas that induces a high glucose level in the blood is the primary cause of diabetes.^[5] Some other factors such as genetic, lifestyle, and viral causes are also responsible for diabetes.^[1] Maintaining the blood glucose level within the normal concentration range (<100 mg dL⁻¹ while fasting) is the key strategy for saving lives and avoiding the associated diseases caused by diabetes.^[1,6] Thus, the development of precise and accurate measurements of glucose concentrations in human body

fluids using low-cost, easy, and portable devices is highly demanded.

Several glucose-sensing devices and methodologies have been developed in the last two decades based on electrochemical and optical techniques.^[7–9] In particular, electrochemical systems caught considerable interest due to their high sensitivity, low limit of detection (LOD), portability, low-cost, easy operation, and good selectivity.^[7] They have been commercialized with great success since the introduction of self-testing blood glucose electrochemical meters in the 1980s.^[7–9] Although an electrochemical glucose sensor allows self-monitoring and point-of-care (POC) testing, issues such as long-term stability, accuracy, and reliability are yet to be resolved. Optical detection systems (e.g., based on fluorescence (FL), colorimetry (CM), surface plasmon resonance (SPR), surface-enhanced Raman scattering (SERS)) have also been developed and are highly competitive. They allow continuous glucose monitoring (CGM) every 1–5 min with high accuracy up to about one week. However, CGMs based on an enzymatic reaction require frequent calibrations (usually 5–8 times a day)^[9–11] and have to be replaced regularly due to the degradation of reagents and the immune response of the body, all circumstances


M. Adeel, K. Asif, F. Rizzolio, S. Daniele
Department of Molecular Sciences and Nanosystems
Ca'Foscari University of Venice
Venezia 30123, Italy

E-mail: muhammad.adeel@unive.it; sig@unive.it

M. Adeel, K. Asif, F. Rizzolio, V. Canzonieri
Pathology Unit
Centro di Riferimento Oncologico di Aviano (CRO) IRCCS
Aviano 33081, Italy

M. M. Rahman
Department of Applied Chemistry
Konkuk University
Chungju 27478, South Korea
E-mail: mahbub1982@kku.ac.kr

V. Canzonieri
Department of Medical
Surgical and Health Sciences
University of Trieste
Trieste 34127, Italy

 The ORCID identification number(s) for the author(s) of this article can be found under <https://doi.org/10.1002/adfm.202106023>.

DOI: 10.1002/adfm.202106023

that lead to an increase in the cost of detection. It must be highlighted that though most of the commercially available electrochemical and optical glucose sensors require a small amount of blood (1 μL) for the measurements, the sample is typically taken from the body by either finger pricking or a thin lancelet implanted subcutaneously. Both methodologies are invasive, cause discomfort and pain after repeated use, and can pose the patient at risks of potential infection or cause tissue damage.^[10–14] Therefore, there has been a continuous effort for developing noninvasive or minimal invasive glucose sensors by modifying the technology and devices or using samples different from blood (e.g., body fluids such as sweat, tears, and urine).^[1,10,15]

Electrochemical and optical glucose sensors can be classified into enzymatic and nonenzymatic. In an electrochemical enzymatic glucose sensor, typically, a glucose oxidase (GO_x) enzyme-modified electrode is used. GO_x acts as a catalyst for the oxidation of glucose, and it is often coupled to nanostructured electrode modifiers such as metal-oxides (MOs) (ZnO , Al_2O_3 , TiO_2 , etc.) and other metal nanostructures, carbon nanocomposites, and hydrogels.^[16–19] These nanostructured materials have a dual function: as electron transporting channels and as matrices onto which GO_x is immobilized. The GO_x enzyme-based commercially available electrochemical glucose sensors suffer from poor environmental stability and involve complex GO_x immobilization processes onto the sensor surface.^[1] Additionally, GO_x loses its catalytic activity at higher (> 8.0) and lower (< 2.0) pH and is affected by the presence of surfactants.^[1,8] These limitations of GO_x triggered researchers to develop nonenzymatic electrochemical glucose sensors. In nonenzymatic electrochemical glucose sensors, biomimetic nanozymes such as metal nanomaterials (e.g., Au, Pt, Ag, Ni, Cu, Co, etc.),^[20] MOs (e.g., NiO , CuO , Co_2O_3 , MnO_2 , ZnO , etc.),^[19] metal sulphides,^[21,22] metal-organic frameworks (MOFs),^[23] metal-azolate frameworks (MAFs),^[24,25] and nanocomposites,^[26] are utilized as electrode modifiers. Most of them catalyse the glucose oxidation in an alkaline condition, which represents an issue since the detection of glucose at physiologic pH would be preferable, especially for direct measurements in blood. Au and Pt-based nanomaterials could catalyse glucose oxidation also at physiological pH, but they are costly and suffer from poisoning effects due to electrochemically generated intermediates.^[27] In addition, Pt nanomaterials, in real biological matrices, display strong protein adsorption ability and poor selectivity toward glucose oxidation due to the interference of other bio-molecules, which leads to unreliable current responses for glucose concentration measurement.^[28]

In enzymatic optical glucose sensors, GO_x is entrapped into nanomaterials together with various recognition elements (e.g., fluorescent dyes, fluorophores-luminescent complexes) that induce optical signals upon glucose oxidation, which can be revealed using different optical methods.^[9,29–31] These devices have also been employed successfully for the detection of glucose directly in body sweat, tears, and saliva. However, also enzymatic optical sensors display the same limitations due to enzyme stability, as outlined above for the electrochemical enzymatic sensors. Therefore, nonenzymatic optical sensors have also been developed.

For both enzymatic and nonenzymatic sensors and for whatever transduction systems, in the last decade MOFs, the subclasses of MOFs, and their composites have attracted significant attention as electrode/support materials and recognition elements.^[24,25] MOFs are hybrid porous materials that are constituted by the metal ions (Mn^+)/cluster Mn^+ in the center, surrounded by organic ligands (Figure 1a).^[32–34] MOFs have been widely used in several fields, including batteries, supercapacitors, solar cells, and sensor technology due to their high surface-to-volume ratio, high porosity, and catalytic activities (Figure 1b).^[35–42] So far, over 20 000 MOFs have already been developed, and many of them have been successfully used not only for glucose sensing but also for the detection of other chemical species such as H_2O_2 , L-cysteine, tryptophan, and glutathione.^[24,25] For the detection of glucose in biological fluids, MOFs have been integrated into electronic devices, microfluidics, and transistors and have allowed achieving high sensitivity, selectivity, and low LODs.^[43,44] The interest of researchers toward MOFs for general sensing applications and in particular for glucose detection has increased steeply as is evident from the number of publications that appeared in the last decade (Figure 1c). This denotes the potential of these materials in the sensor field.^[45]

In spite of the importance of these materials, to the best of the authors' knowledge, no review summarizing the progress of MOFs and their derivatives for glucose sensing is reported in the literature. This paper aims at providing a comprehensive overview of the state-of-art of MOFs, their subclasses and composites, as well as MOF-derived materials to build enzymatic and nonenzymatic electrochemical, optical, transistors, and microfluidics glucose sensors. Additionally, the general design and synthesis methods of MOFs and the general electrochemical and optical glucose-sensing mechanism using MOFs are discussed by highlighting the current challenges and future perspectives.

2. Design of MOFs for Glucose Sensors

MOFs are flexible and porous (ranging from micropore to mesopore scale) materials with zeolite-type structures.^[46,47] Various methods have been developed for the synthesis of MOFs, including hydro (solvo) thermal, diffusion, microwave, ultrasound, and electrochemical approaches.^[48,49] MOFs can be synthesized in different shapes, dimensions, functionalities, high surface area (from 1000 to 10 000 $\text{m}^2 \text{g}^{-1}$), and porosity (down to 9.8 nm pore diameter) by controlling the synthesis methods and conditions (e.g., temperature, pressure, solvents, pH, reaction time).^[50,51] The high surface area and porosity of MOFs allow the easy diffusion, adsorption, and entrapment of guest molecules into their infinite and ordered frameworks. These outstanding characteristics widen the application of MOFs, MOF composites, and MOF-derived materials in various technological fields.^[32]

For biosensing applications, the chemical stability of MOFs in aqueous media over a wide pH range and, for electrochemical based devices, high electrical conductivity are prerequisites for reliable data acquisition.^[24,25,52] However, most

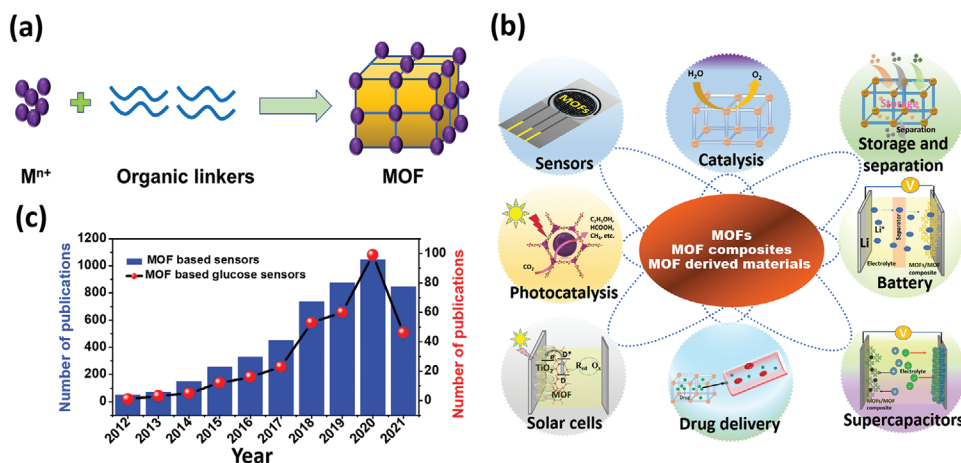


Figure 1. a) Schematic illustration of the preparation of MOFs, b) applications of MOFs, and c) number of publications of MOFs-based sensors and glucose sensors from 2012 to July 2021; source: Web of Science.

of the MOFs are unstable in an aqueous medium and insulating at low bias. Ding et al. comprehensively summarized the approaches and the progress in designing and synthesizing stable MOFs toward a broader range of applications.^[53] For glucose sensing the issues that need to be considered depend on either the transduction system employed and the role played by MOFs themselves (i.e., enzymatic or nonenzymatic oxidation of glucose), as schematized in **Figure 2** and highlighted below:

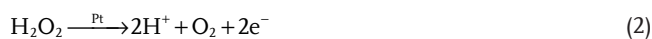
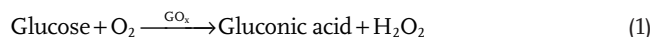
- Utilization of hydrophobic and N-donor linkers (e.g., pyrazolate, imidazolate, 1,2,4-triazolate, etc.) in order to impart to the materials distinctive tolerance to aqueous solutions at the working pH values (typically neutral and basic media). These characteristics were achieved, for example, by Co-MAF based on 2-ethylimidazole linker for glucose sensing.^[24,25,52] Alternatively, tolerance to water solutions can also be achieved by post-synthetic modification with long-alkyl substituents, or hydrophobic surface treatment of MOFs to protect from water without the loss of porosity.^[53,54] A scheme that closely follows this idea was proposed by Lopa et al., who developed MAF 4-Co^{II} using 2-methylimidazole hydrophobic linkers for nonenzymatic glucose sensing.^[24,53]
- Selection of chemically inert Mn⁺-compounds, characterised by low toxicity and low-cost, which are important aspects for the environmental sustainability and commercial availability of the sensors. This is the case, for example, of several Cu-MOFs and Fe-MOFs, which in addition, present low toxicity.^[58,63]
- Utilization of two or more Mn⁺/cluster Mn⁺ to form stable secondary building unit (SBU), which could form a strong coordination bond with the ligands and increase the inertness and hydrophobicity of the final product, as reported by Patra et al. in a work dealing with a Pt NPs and Fe-MOF (iron(III) trimesate or MIL-100(Fe)) nanocomposite for the immobilization of GO_x.^[58]
- Use of redox active Mn⁺/cluster Mn⁺ with lower redox potential to avoid interference due to species present in real samples that oxidize at higher redox potentials, examples include the use of copper, cobalt and nickel.^[24,25]

- Improve the selectivity of the material by direct insertion of size-matching ligands as brackets into the pores of MOFs via de novo synthesis, which splits the large cage or channel space into smaller segments for GO_x entrapment.^[53] These aspects have been taken into consideration and have led, with more or less success, to the development of various MOFs-based sensors for the determination of glucose, as will better appear from the examples reported in this review article.

3. Evolution of Different Generations and Mechanism of MOF-Based Electrochemical Glucose Sensors

3.1. Evolution of Electrochemical-Based Glucose Sensors

Electrochemical transduction system-based glucose sensors attained the highest success because of their low-cost device fabrication, reliable output signal, and ease to use for diabetic patients. In this method, an electrical signal is applied (current and voltage) as input, and the output current, voltage, or resistance changes are measured to quantify the glucose concentration.^[55] In 1962, Leland C. Clark first introduced an electrochemical glucose sensing system based on GO_x modified Pt electrode,^[1,8] relying on the following reaction mechanism and denoted the first-generation of the glucose sensors (**Figure 3**)



Later, progression began of the first-generation glucose sensors by replacing GO_x with glucose-1-dehydrogenase (GDHs).^[1] GO_x utilizes O₂ as the external electron acceptor, whereas GDHs use pyrroloquinoline quinone and flavin adenine dinucleotide as the cofactor for the oxidation of glucose in biological fluids. Although GDHs-based amperometric

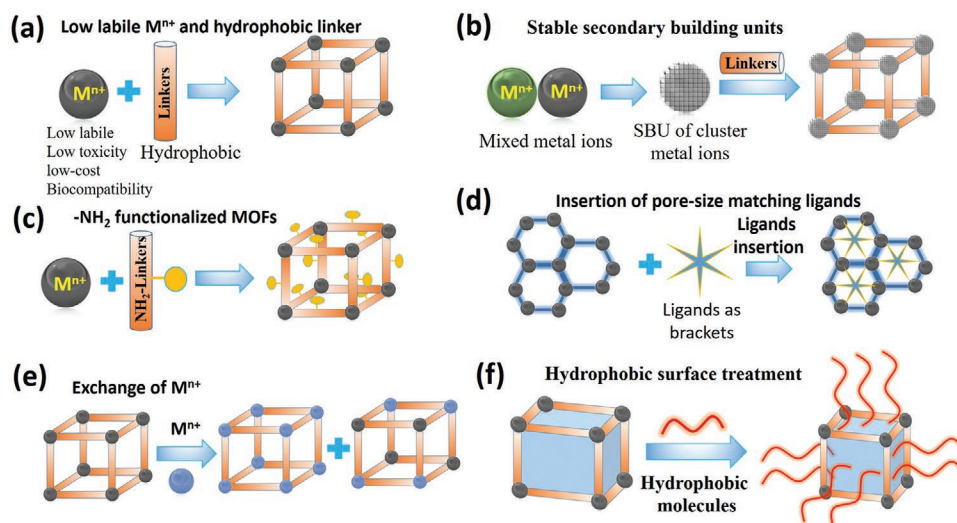


Figure 2. Schematic illustrations of routes to build chemically stable MOFs.

biosensors are advantageous in being able to be operated at lower detection potentials than the first-generation GO_x -based sensors, and their performance is not influenced by the O_2 level in the analyte solution, they suffer from several drawbacks and result in less popularity compared with GO_x utilized in glucose biosensing.^[55] Subsequently, a second-generation of glucose sensor was developed, utilizing non-physiological redox mediators (e.g., methylene blue, indigo disulfonate, ferrocenemethanol, benzyl viologen, etc.) to transporting electrons from the enzyme to the sensing electrode (Figure 3).^[56] This requires O_2 free biological fluids to eliminate the competition between the mediator and O_2 . Moreover, a mediator must be stable indefinitely during the redox processes for continuous glucose oxidation. This limitation inspired the development of a third-generation glucose

sensors based on the direct charge transfer between the enzyme and the sensing electrode, eliminating the necessity of both mediator and O_2 (Figure 3).^[55,56] All these generations (first to third) of glucose sensors utilize enzymes, suffering from the reliability of measurement due to the low-stability of enzymes and the chemical deformation during the manufacturing process, storage, and use.^[1,55,56] Therefore, a large number of nanomaterials were developed, which served as biomimetic enzymes (also defined nanozymes) for the enzymeless oxidation of glucose. They are classified as fourth-generation glucose sensors (Figure 3).^[1,55,56] All the generations of glucose sensors require the use of novel nanomaterials to serve as an electron transporting channel, enzyme immobilization matrix, and nanozyme. For all these purposes, MOFs are very attractive materials.

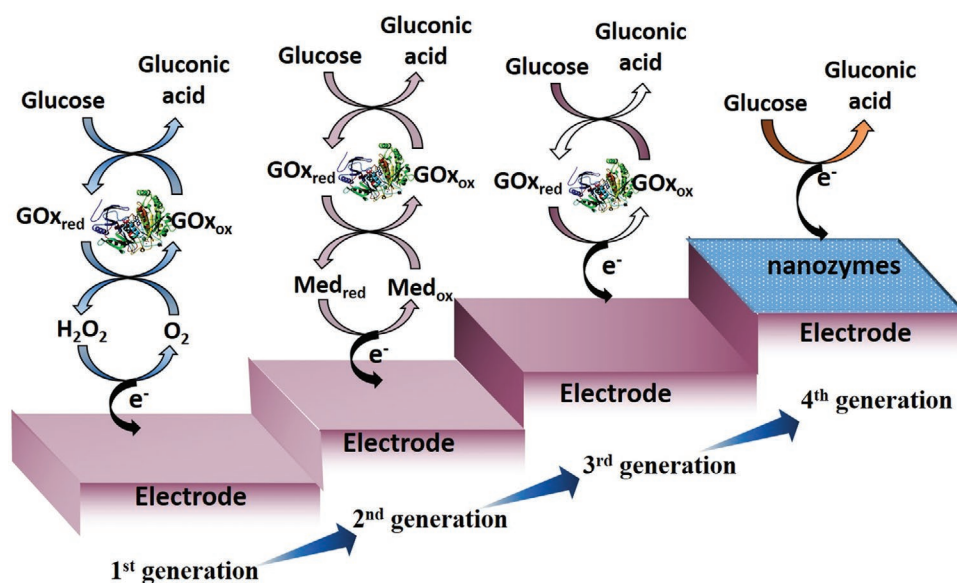


Figure 3. Schematic illustration of working principles for different generations of electrochemical glucose sensors.

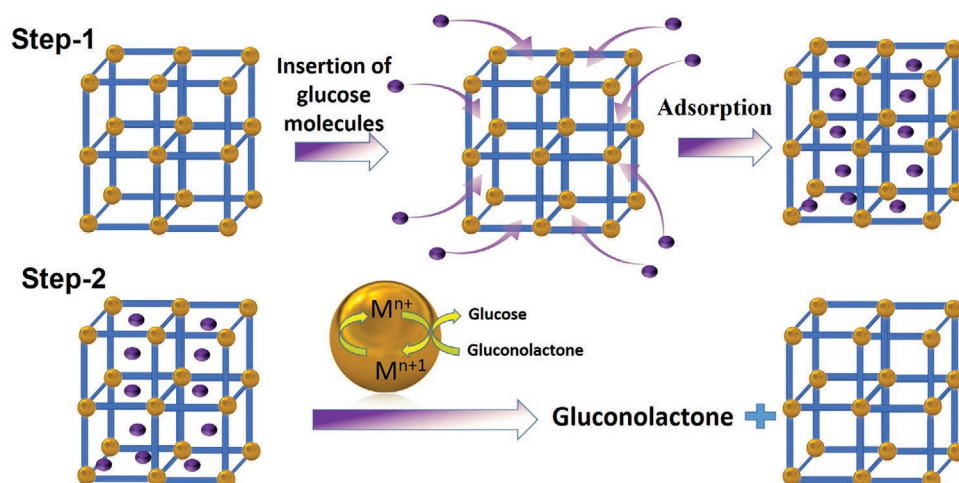


Figure 4. Schematic illustration of nonenzymatic sensing through metal–organic frameworks.

3.2. Mechanism of MOF-Based Nonenzymatic Glucose Sensors

The electrochemical redox activity of Mn^{+} /cluster Mn^{+} in the MOFs can mediate the redox reaction of various molecules. For this, the diffusion of the analytes close to the Mn^{+} /cluster Mn^{+} or into the pore of MOFs is essential for efficient mediated redox reaction. The mechanism of a MOF-based nonenzymatic electrochemical glucose sensor can be considered a two steps process (**Figure 4**). In the first step, glucose molecules (size about 1 nm) enter the pore of MOFs (pore size up to 9.8 nm) and eventually adsorbed on the active center;^[50] in the second step, Mn^{+} /cluster Mn^{+} is oxidized upon the applied potential and reduced back by the oxidation of glucose into gluconolactone. This induces to increase in the oxidation current with the increase of the concentration of glucose.^[24,25]

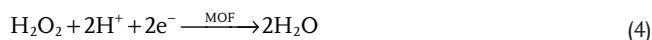
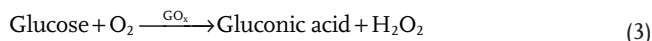
3.3. Mechanism of MOF-Based Enzymatic Glucose Sensors

For an enzymatic electrochemical glucose sensor, pristine MOFs and their composites are generally used for the entrapment of GO_x , process facilitated by the large pores of MOFs.^[57,58] Upon the application of a suitable potential, glucose is oxidized to gluconic acid induced by GO_x , thus enabling glucose detection (see reactions below and **Figure 5a**). However, the physical entrapment of the bulky GO_x ($6.0 \times 5.2 \times 77 \text{ nm}^3$)^[59] into the pores of MOFs can deteriorate their structure, consequently the stability of sensors. To avoid this problem, a large number of MOFs with free guest-accessible functional groups (e.g., $-NH_2$, $-SO_3H$, $-NO_2$, $-NHCO-$ or $-NHCONH-$, etc.) have been developed.^[60] Thus, GO_x can be immobilized onto the surface or into the pores of MOFs by covalent interaction with the functional moieties (e.g., $-NH_2$ and/or $-COOH$), enabling the electrochemical oxidation of glucose to gluconic acid (**Figure 5a**). Surprisingly, no report is available concerning the development of enzymatic sensors based on functionalized pristine MOFs. This is conceivably due to the intrinsic characteristics of MOFs.

The low conductivity of pristine MOFs is another factor that limits the performance of GO_x -based MOF sensors. To deal with

this drawback, several types of MOFs composites, containing metal- and carbon-based materials, have been developed.^[57]

MOF composites have been utilized for the oxidation of glucose on a mimetic multi-enzyme system, in which MOF acted as a secondary biomimetic catalyst for H_2O_2 reduction.^[61] The immobilized or entrapped GO_x into the MOFs composites can catalyse the oxidation of glucose with the production of gluconic acid and H_2O_2 . The latter is reduced to H_2O mediated by the peroxidase-like activity of a specific MOF in the composite (as shown in the following reactions and **Figure 5b**)



4. MOF-Based Nonenzymatic Electrochemical Glucose Sensors

4.1. Pristine MOFs

For a nonenzymatic glucose sensor, the electrode modifiers should act as biomimetic enzymes. To this purpose, MOF systems with various Mn^{+} /cluster Mn^{+} ($M = Cu, Ni, Co, Fe$, etc.) have been developed for the construction of electrochemical glucose sensors.^[62–64] Some selected examples are outlined below, while others based-MOFs and exploiting similar reaction mechanisms are enumerated in **Table 1** together with the main analytical performance.

Cu-based pristine MOFs have been widely investigated for glucose sensing due to their lower redox potential (ranging between 0.1 and 0.5 V vs SCE or Ag/AgCl, reference electrodes) and high selectivity without the interferences due to maltose, fructose, sucrose, ascorbic and uric acid, and other biomolecules. Furthermore, Cu is a nontoxic and low-cost element. Sun et al. developed the hydrothermally Cu-based MOF, $[Cu_2(BTC)Cl(H_2O)_4]$,^[64] which was employed to modify a conventional glassy carbon electrode (GCE), using Nafion as a binder. The as-prepared sensor exhibited electrocatalytic

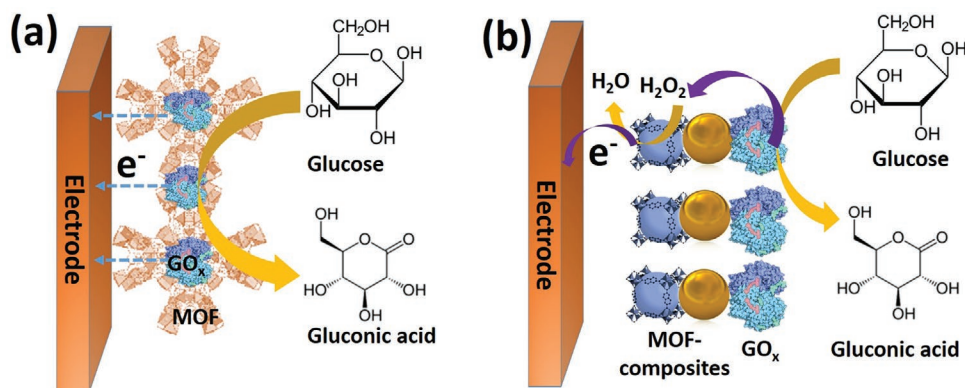


Figure 5. Schematic illustration of different architectures of enzymatic glucose oxidation mechanism based on MOFs and MOF composites: a) physical entrapment and covalent immobilization of GO_x into MOFs and b) peroxidase mimicking of MOFs.

activity for the oxidation of glucose in basic solution induced by the electrochemically generated Cu³⁺ from the Cu²⁺ of the Cu-MOF. The sensor displayed a linear range from 0.06×10^{-6} to 5000×10^{-6} M, a sensitivity of $89 \mu\text{A cm}^{-2} / \times 10^{-3}$ M, and a LOD of 0.01×10^{-6} M. It was applied for the detection of glucose in urine spiked samples. Wu et al. used a hydrothermally synthesized Cu-MOF (HKUST-1) for the modification of a carbon paste electrode (CPE), made by mixing graphite powder (10%) and paraffin (30%), the latter as a binder.^[63] The high surface area ($491.59 \text{ m}^2 \text{ g}^{-1}$) and porosity (average size of pores of 0.498 nm) of the Cu-MOF provided a catalytic activity for glucose oxidation in NaOH solution (pH 13.0). The oxidation process again involved a Cu³⁺/Cu²⁺ redox couple. Calibration plots obtained with the Cu-MOF/CPE sensor showed two linear ranges, between 5×10^{-6} and 3910×10^{-6} M and 3910×10^{-6} and 10950×10^{-6} M, and a LOD of 0.11×10^{-6} M. The response time to concentration changes was very short, equal to 0.5 s. The suitability of the sensor in real world application was assessed in diluted serum samples. Cu-based MOFs are also promising for the development of multi-analyte sensors by exploiting the formation of multiple redox pairs Cu²⁺/Cu⁺ and Cu³⁺/Cu²⁺, characterized by different redox potentials. Taking advantage of the latter characteristics, Zhang et al. solvothermally synthesized a highly porous and structurally stable 3D Cu-MOF (MOF-14) for the modification of a CPE, which was then applied for the detection of glucose and H₂O₂.^[62] The enzymeless detection of glucose and H₂O₂ was performed in basic and neutral solutions, respectively, by exploiting the Cu³⁺/Cu²⁺ and Cu²⁺/Cu⁺, respectively. The amperometric detection of glucose was performed at 0.7 V, and the calibration plots revealed two linear ranges, 5×10^{-6} – 45×10^{-6} M and 45×10^{-6} – 2800×10^{-6} M,

and a LOD of 1×10^{-6} M. Unfortunately, no application of the sensor in real samples or its suitability for the simultaneous detection of both analytes were assessed.

Ni or Ni-based MOFs have also been used to detect glucose. In all these systems, the electrocatalytic oxidation of glucose involved the Ni³⁺/Ni²⁺ redox couple. Chen et al. developed Ni-MOF microspheres (Ni-BTC) and NiO derived from Ni-MOFs to modify the electrode surface for non-enzymatic detection of glucose in an alkaline medium.^[65] It was found that the Ni-BTC sensor displayed higher analytical performance than that of the NiO derived from Ni-BTC. This was attributed to a faster heterogeneous charge transfer occurring at the Ni-BTC-modified electrodes. In both cases, two linear concentration ranges were found (5×10^{-6} – 3000×10^{-6} M and 3500×10^{-6} – 6000×10^{-6} M with sensitivity of $932.68 \mu\text{A cm}^{-2} / \times 10^{-3}$ M and $273.04 \mu\text{A cm}^{-2} / \times 10^{-3}$ M, respectively).^[65] It must be considered the latter behavior, with a lower sensitivity at high glucose concentrations, is common for highly porous materials, as is the case of MOFs-derived sensors. This phenomenon was explained to be essentially due to hindered diffusion within the pores for both glucose and gluconolactone. Lopa et al. solvothermally synthesized a Ni-MOF (Ni₂(dihydroxyterephthalic acid, also known as CPO-27-Ni^{II}) with high surface area ($950 \text{ m}^2 \text{ g}^{-1}$) (Figure 6a).^[66] Also in this case, the CPO-27-Ni^{II} modified-GCE exhibited two dynamic ranges for the electro-oxidation of glucose in an alkaline medium. The operational stability of the sensor was low (stable up to 500 s) due to the separation of Ni(OH)₂ from the MOF structure. However, the stability was high enough for the development of disposable-type sensors.^[66]

Table 1. Analytical performance of nonenzymatic electrochemical glucose sensors based on pristine-MOFs.

Electrode material	Technique	Linear range [$\times 10^{-6}$ M]	LOD [$\times 10^{-6}$ M]	Sensitivity [$\mu\text{A cm}^{-2} / \times 10^{-3}$ M]	Potential [V]	Ref.
Cu-MOF	AMP	5–10 950	0.11	–	0.45	[63]
Cu-MOF	DPV	0.06–5000	0.01	89	–	[64]
Cu-MOF	AMP	10–1900	–	273	0.60	[72]
Ni-MIL-77	AMP	1–500	0.25	1.542	0.60	[73]
Co-MOF	AMP	5–900	1.6	169	0.40	[74]

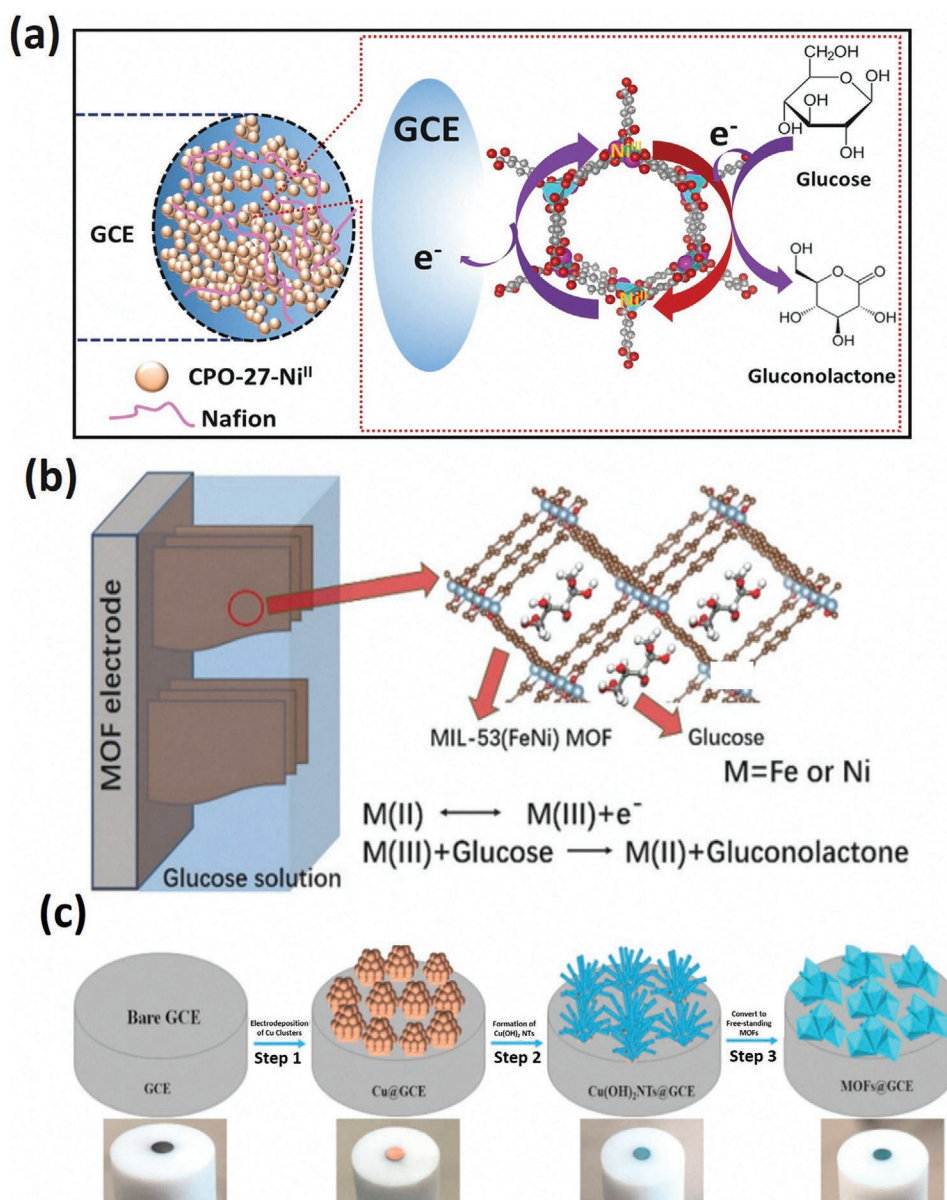


Figure 6. a) Mechanism of glucose oxidation at the CPO-27-Ni^{II}/GCE sensor. Reproduced with permission.^[66] Copyright 2018, Elsevier. b) Mechanism of glucose oxidation at the MIL-53(NiFe)/Ni sensor. Reproduced with permission.^[67] Copyright 2019, Royal Society of Chemistry. c) Schematic illustration to develop binder-free Cu-MOF/GCE. Reproduced with permission.^[68] Copyright 2018, Elsevier.

Bimetallic or mixed-metallic MOFs were developed to make stronger the coordination bond between metal ions and ligands and to increase the inertness and hydrophobicity of the final product.^[53] To avoid problems related to the low conductivity of MOFs and the use of insulating Nafion or paraffin binders, some strategies involving the direct growth of MOFs onto the electrode surface were adopted. For example, Zhang et al. prepared a mixed Ni²⁺/Fe²⁺ MOF (MIL-53(NiFe)), directly grown on a Ni foam (Figure 6b), the latter acting as an electrode substrate.^[67] This MIL-53(NiFe)/Ni sensor worked in alkaline media and showed good performance in terms of sensitivity (41.95 mA cm⁻²/× 10⁻³ M), LOD (0.67 × 10⁻³ M), and selectivity (i.e., negligible interferences due to several biological molecules, including acetaminophen, ascorbic acid, dopamine,

uric acid, sucrose, fructose, L-cysteine, and folic acid). These analytical characteristics can be ascribed to the higher number of active sites (i.e., electrochemically formed Ni³⁺ and Fe³⁺ in MIL-53(NiFe)/Ni) toward the oxidation of glucose, as well as to the molecular sieve effect of the MIL-53(NiFe) MOF, which hinders diffusion of interferences toward the active sites. Noteworthy, the sensor was electrochemically stable for up to 18 days without any noticeable variation of current for glucose oxidation. A binder-free Cu-MOF-modified GCE electrode was developed by Shahrokhian et al.^[68] In this case, the fabrication involved a first stage in which Cu was electrodeposited onto the GCE. Subsequently, Cu was converted into Cu(OH)₂ nanotubes (NT) by both chemical and electrochemical anodization in an alkaline solution. Finally, Cu-MOF (Cu-BTC) was prepared by

reacting $\text{Cu}(\text{OH})_2\text{-NT}$ with H_3BTC ($\text{C}_9\text{H}_6\text{O}_6$) linker (Figure 6c). This self-supported Cu-MOF/GCE worked in an alkaline medium providing a linear range, response time, and LOD of $2\text{--}4000 \times 10^{-6}$ M, 1.6 s, and 0.6×10^{-6} M, respectively.

Other than Cu and Ni-based MOFs, binder-free Co-based MOFs were also developed for nonenzymatic detection of glucose.^[69–71] Li et al. hydrothermally prepared a Co-MOF ($[\text{Co}_2(\text{OH})_2\text{C}_8\text{H}_4\text{O}_4]$) nanosheets (NS) array onto a Ni foam.^[69] The oxidation of glucose was performed in an alkaline solution and displaying good analytical performance (i.e., sensitivity, LOD, linear range, and response time were: $10\ 886\ \mu\text{A cm}^{-2} \times 10^{-3}$ M, 1.3×10^{-9} M, 1×10^{-6} to 3000×10^{-6} M, and <5 s, respectively). However, in the alkaline medium, the stability of the sensor was low due to the weak interaction between Co^{2+} and the organic linker.

Other articles report on a variety of pristine Cu-MOF, Ni-MIL-77, and Co-MOF-based electrochemical enzymeless glucose sensors.^[63,64,72–74] The mechanisms involved are similar to those described above, while their analytical performances, including linear range, LOD, sensitivity, and applied potential, are summarized in Table 1. In addition, most of the MOFs-based sensors here considered were employed for the detection of glucose in real matrix, such as serum, plasma, urine, and even in food samples.

4.2. Subclasses of MOFs

MAFs or zeolite imidazolate frameworks (ZIF)) are one of the evolving subclasses of MOFs, exhibiting directional coordination ability between azolate ligands (e.g., tetrazolates, pyrazolates, triazolates, imidazolates, etc.) and metal ions.^[75] Imidazolate linkers-based MAFs are advantageous to obtain a relatively larger pore size due to their longer bridging length. The tuneable pores and the inert/hydrophobic inner/outer surface of MAFs are attractive for the development of high-performance and chemically stable electroanalytical devices with high reproducibility. Recently, MAFs or ZIFs and their composites have attracted wide interest in the development of enzymeless electrochemical glucose sensors. Lopa et al. developed a nonenzymatic glucose sensor using a solvothermally synthesized and highly crystalline Co-MAF (MAF-4- Co^{II} or $\text{Co}(\text{mim})_2$), (Figure 7a).^[25] The Nafion binder containing as-prepared MAF-4- Co^{II} -modified GCE showed electrochemical stability for glucose oxidation for up to 1 h in NaOH solution. As for other MOF-based sensors, two dynamic ranges, i.e., from 2×10^{-6} to 50×10^{-6} M and 100×10^{-6} to 1800×10^{-6} M were found, with a lower sensitivity (i.e., $30.95\ \mu\text{A cm}^{-2} / \times 10^{-6}$ M, compared to $990.90\ \mu\text{A cm}^{-2} / \times 10^{-3}$ M) at higher glucose concentrations. The LOD was 0.60×10^{-6} M. Improvements in the performance of MAF-based glucose sensors were achieved by using ultra-thin 2D structures, which allowed an easier accessibility of the analyte toward the catalytically active sites of the sensor.^[16] Having this in mind, our group opening a new possibility of MAFs applications, preparing a 2D NS of Co-MAF (MAF-5- Co^{II}) by a simple hydrothermal method. The MAF material with Nafion binder were employed to modify commercially available screen-printed electrodes (SPEs) (Figure 7b).^[24] The as-prepared MAF-5- Co^{II} /SPE could detect

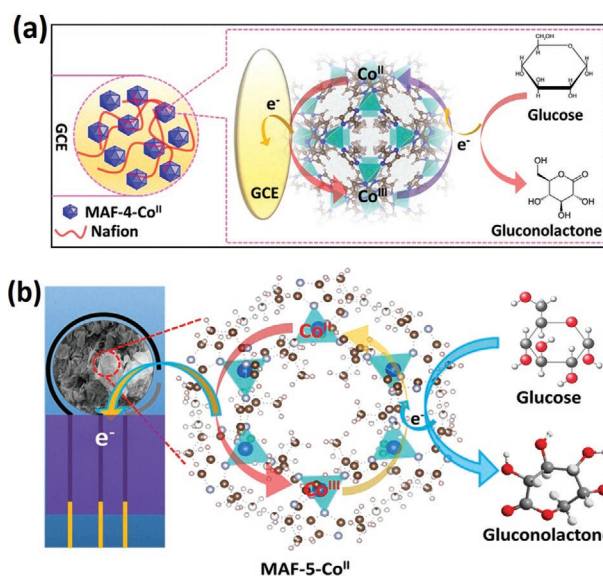


Figure 7. a) Schematic of the plausible mechanism for glucose oxidation at MAF-4- Co^{II} /GCE sensor for glucose oxidation in $\text{NaOH}(\text{aq})$. Reproduced with permission.^[25] Copyright 2019, Elsevier. b) Schematic of the plausible mechanism of glucose oxidation at MAF-5- Co^{II} /SPE sensor at physiological pH. Reproduced with permission.^[24] Copyright 2021, Springer.

glucose nonenzymatically in both alkaline media and at physiological pH, again providing two linear concentration ranges (from 62.80×10^{-6} to 180×10^{-6} M, and from 305×10^{-6} to 8055×10^{-6} M) and a LOD of 0.25×10^{-6} M. In both media, the glucose oxidation process occurred through the formation of the $\text{Co}^{\text{II}}/\text{Co}^{\text{III}}$ redox pair in the MAF system.

4.3. MOFs and MAFs/ZIFs Composites

As mentioned in Section 2, the low electrical conductivity of MOFs is an issue that can limit the practical applications of pristine MOFs as electrocatalysts for glucose sensing.^[76,77] This drawback was overcome by using highly conductive nanomaterials such as graphene, carbon nanotubes (CNTs), metal nanoparticles and activated carbon loaded or encapsulated in MOFs.^[78–81] Therefore, MOFs and MAFs or ZIF act as templates to load a variety of nanomaterials.^[82,83] For example, Wang et al. prepared a hierarchical 3D flower-like Ni-MOF (nickel(II)-(Ni(TPA))) through a simple solvothermal method.^[84] Subsequently, single-wall carbon nanotubes (SWNTs) together with chitosan (CS) were incorporated into the Ni-MOF by applying ultrasounds. CS acted as a dispersing and binding agent (Figure 8a). The as-prepared Ni-MOF-SWNT-CS modified GCE showed significantly enhanced catalytic activity for the oxidation of glucose in alkaline media compared to the pristine Ni-MOF and SWNT, induced by the cooperative effect of electrocatalytic Ni-MOF and the high electrical conductivity of SWNT. The composite sensor displayed a linear range from 20×10^{-6} M to 4.4×10^{-3} M, a LOD of 4.6×10^{-6} M, and fast response (<5 s). In another report, Chen et al. prepared graphene nanosheets (GS)

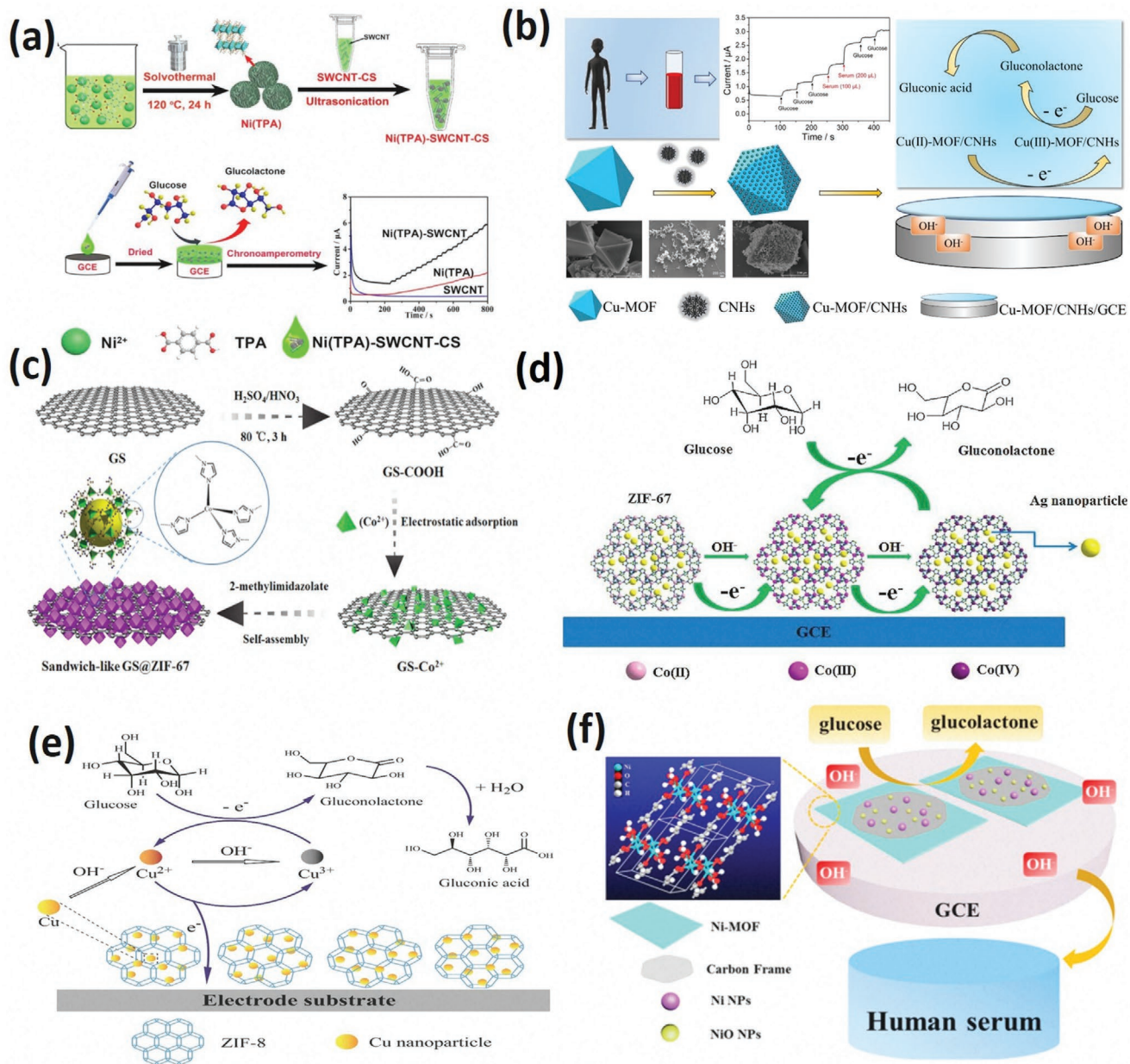


Figure 8. a) Schematic of the synthesis of Ni-MOF-SWCNT-CS composite, electrode fabrication, reaction mechanism, the corresponding amperometric signals for glucose oxidation. Reproduced with permission.^[84] Copyright 2019, Elsevier. b) Schematic of the fabrication of Cu-MOF/CNHs/GCE, scanning electron micrographs (SEM), and the reaction mechanism for glucose oxidation. Reproduced with permission.^[87] Copyright 2020, Elsevier. c) Schematic illustration of the synthesis of sandwich-like graphene@ZIF-67 heterostructure. Reproduced with permission.^[85] Copyright 2019, American Chemical Society. d) Schematic of the reaction mechanism for glucose oxidation at Ag@ZIF-67 sensor. Reproduced with permission.^[104] Copyright 2018, Elsevier. e) Schematic of the reaction mechanism for glucose oxidation at Cu-in-ZIF-8 sensor. Reproduced with permission.^[105] Copyright 2016, Elsevier. f) Schematic of the Ni-MOF/Ni/NiO/C/GCE sensor for glucose detection in human serum sample. Reproduced with permission.^[88] Copyright 2017, American Chemical Society.

sandwiched Co-based ZIF ($[\text{Co}(\text{mim})_2]_n$ or ZIF-67) nanohybrids (Figure 8b).^[85] The GS@ZIF-67 hybrids with an ordered nanostructure showed better catalytic activities toward glucose oxidation compared to the pristine ZIF-67. This is conceivably due to the synergistic effect of more accessible catalytically active sites of ZIF-67 and the high electrical conductivity of GS. This GS@ZIF-67 hybrids-based nonenzymatic glucose sensor showed high sensitivity of $1521.1 \mu\text{A cm}^{-2}/\times 10^{-3} \text{ M}$

with a linear range between 1×10^{-6} and $805.5 \times 10^{-6} \text{ M}$ and LOD of $0.36 \times 10^{-6} \text{ M}$ ($S/N = 3$). Similarly, some other carbon materials based MOF composites such as Ni-MOFs/CNTs^[86] and Cu-MOF/carbon nanohorns (CNHs) (Figure 8c)^[87] were reported for nonenzymatic glucose sensing, which showed better analytical performance for glucose sensing compared to the corresponding bare MOFs counterpart. The analytical performance of these materials is also included in Table 2.

Table 2. Analytical performance of nonenzymatic electrochemical glucose sensors based on MOF composites.

Electrode material	Linear range [$\times 10^{-6}$ M]	LOD [$\times 10^{-6}$ M]	Sensitivity [$\mu\text{A cm}^{-2}/\times 10^{-3}$ M]	Potential [V]	Ref.
Ni-MOF/SWCNT	20–4400	4.6	–	0.55	[84]
Ni-MOF/CNTs	1–1600	0.82	13 850	0.60	[86]
Cu-MOF/CNHs	0.25–1200	0.078	–	0.32	[87]
Ni-MOF/Ni/NiO/C	4–5664	0.8	367.45	0.65	[88]
Ag@TiO ₂ @ZIF-67	48–1000	0.99	78.8	0.40	[89]
CuO NPs/Ce-MOF	0.005–8600	0.002	2058.5	0.55	[90]
Boron nitride/MOF	10–900	5.5	18 100	0.60	[91]
Cu ₂ O@ZIF-67	10–10 000 and 10 000–16 300	6.5	307.02 and 181.34	0.55	[92]
TiO ₂ /ZIF-8	–	0.08	–	-0.45	[93]
AuNP/Ni-MOF/Ni/NiO	0.4–900	0.1	2133.5	0.65	[94]
Ni ₃ (PO ₄) ₂ @ZIF-67	1–4000	0.7	2783	0.45	[95]
Co ^{II} -MOF/Acb	5–1000	1.7	255	0.55	[96]
Au@Ni-MOF	5–7400	1.5	1447.1	0.55	[97]
CuO/Cu-MOF	1–600	0.33	33 950	0.65	[98]
Co ₃ O ₄ @ZIF-8	5–800	0.13	0.520	0.59	[99]
Ni/Co-MOF	0.1–1400	0.047	2.08	0.42	[100]
Ag NPs/MOF-74 (Ni)	10–4000	4.7	1.29	0.65	[101]
Ni-MOF	2–2000	0.1	27 900	0.65	[102]
Cu NWs/MOF/GO	20–26 600	7	0.007	0.30	[103]

The incorporation of metal nanostructures into MOFs and their subclasses can enhance the catalytic activity of glucose oxidation thanks to the synergetic effects of the various components and to the fact that they prevent the material aggregation, thus maintaining the high surface area and more catalytic active sites. Meng et al. developed a series of Ag@ZIF-67 (Co-based MOF) nanocomposites through a sequential deposition-reduction method by varying the Ag loading amount (from 0% to 0.5%) (Figure 8d).^[104] A GCE was modified with the as-prepared Ag@ZIF-67 composites by using a Nafion binder. The results revealed that the response time of the sensor decreased, and the sensitivity increased with increasing the amount of Ag loading into ZIF-67. The optimized Ag@ZIF-67/GCE sensor, with an Ag content of 0.5%, provided the following analytical characteristics: dynamic range of 2×10^{-6} – 1000×10^{-6} M, sensitivity of $0.379 \mu\text{A cm}^{-2}/\times 10^{-6}$ M, LOD (0.66×10^{-6} M), and good stability and selectivity. In another report, Shi et al. encapsulated Cu nanoparticles (NPs), having sizes ranging from 2.5 to 5 nm, into ZIF-8 (Cu-in-ZIF-8). The latter was used to modify SPE systems for the detection of glucose in NaOH solution (Figure 8e).^[105] Compared to the Cu NPs loaded ZIF-8 (Cu-on-ZIF-8), the Cu-in-ZIF-8 exhibited higher activity and better stability toward glucose oxidation. This can be ascribed to the uniform distribution with a narrow size range of Cu NPs in Cu-in-ZIF-8, which provides plenty of active sites for the electrocatalytic oxidation of glucose. In contrast, Cu-on-ZIF-8, induced to agglomerate the NPs and reduced the electrocatalytic active sites for the oxidation of glucose.

Metal/MO composites loaded MOFs were also reported for nonenzymatic glucose sensing. For example, Shu et al. prepared a Ni-MOF/Ni/NiO/C nanocomposite by one-step calcination method (Figure 8f).^[88] The as-prepared Ni-MOF/Ni/NiO/C

nanocomposite modified GCE displayed better catalytic activity toward glucose oxidation compared to the pristine Ni-MOF and provided LOD and sensitivity of 0.8×10^{-6} M and $36745 \text{ mA cm}^{-2} \text{ M}^{-1}$, respectively. The better performance of the Ni-MOF/Ni/NiO/C nanocomposite was attributed to the higher conductivity of the composite materials with respect to the pristine MOFs. Arif et al. prepared another nanocomposite of Ag@TiO₂@ZIF-67 (Co-based MOF).^[89] The ZIF-67 acted as the chief catalyst for the oxidation of glucose, while Ag@TiO₂ cooperatively enhanced the electron transfer process. An Ag@TiO₂@ZIF-67-modified GCE showed improved analytical performance and high stability. Exploiting similar cooperative functions, a variety of MOF-nanocomposites was developed for glucose sensing, and they showed enhanced sensing performance compared to their corresponding pristine MOFs. The various types of MOFs-composites sensors together with their analytical performance are summarised in Table 2.^[86,87,96,88–95]

4.4. MOF Derived Materials

MOFs can serve as precursors or template for the preparation of new nanomaterials through pyrolysis and chemical decomposition.^[106] Several nanomaterials, for examples MOs (CuCo₂O₄, NiCo₂O₄-NiO), and composites, including carbon based materials, (Fe₃O₄@C/Cu, Cu/Ni/C, Cu/N/C, NiO-NiCo₂O₄@polypyrrole, etc.) were developed for sensing and other electrochemical applications (super cap, batteries and gas separation purposes).^[106–110] Recently, nanomaterials derived from MOFs showed promising aspects for electrochemical glucose sensing due to their high surface area, improved chemical stability, high electrical conductivity, and tunable

porosity. For example, Luo et al. prepared hierarchical CuO nanospheres derived from a Cu-MOF by thermal decomposition (Figure 9a).^[111] The porous hierarchical CuO nanospheres with controllable porosity and surface area showed better glucose sensing properties in an alkaline solution than hierarchical CuO clusters. The sensing mechanism of this sensor involves the oxidation of glucose by the electrochemically generated CuOOH in an alkaline medium. The analytical performance resulted in a linear range of $0\text{--}6.535 \times 10^{-3}$ M, a sensitivity of $806.1 \mu\text{A cm}^{-2}/\times 10^{-3}$ M, and a LOD of 0.15×10^{-6} M. The sensor was tested in artificial saliva containing glucose concentrations in the range from 5×10^{-6} M– 1.165×10^{-3} M. This kind of sensor promises applications for the noninvasive detection of glucose.

The development of bimetallic oxides derived from MOFs can represent another effective strategy to enhance the sensitivity of glucose detection. Yang et al. developed an electrochemical glucose sensor based on MOF-derived hollow CuCo_2O_4 polyhedron/porous reduced graphene oxide (PrGO) composites, prepared by thermolysis of Cu-Co-ZIFs and PrGO (Figure 9b).^[109] The $\text{CuCo}_2\text{O}_4/\text{PrGO}/\text{GCE}$ sensor showed synergistic oxidation of glucose to gluconolactone induced by the reduction of electrochemically generated Cu^{3+} and Co^{3+} to Cu^{2+} and Co^{2+} , respectively, in an alkaline medium. The role of PrGO in the composite is to enhance the conductivity. The analytical performances of the sensor were: sensitivity $2426 \mu\text{A cm}^{-2}/\times 10^{-3}$ M, linear range over $0.5 \times 10^{-6}\text{--}3354 \times 10^{-6}$ M, a response time <3 s, and LOD of 0.15×10^{-6} M.

Carbon materials (e.g., porous carbon, graphene, etc.) incorporating metal and MO composites derived from MOFs are promising electrocatalysts for glucose sensing. The electrooxidation of glucose, catalyzed by metal and MO, can be enhanced by the faster electron transfer processes that occur within the carbon materials. Xiao et al. prepared a metal/MO@carbon composite (M/MO@C) (M = Ni, MO = CuO, Cu_2O , and NiO) by the direct carbonization of bimetallic Cu/Ni-MOF.^[112] A M/MO@C-modified GCE sensor exhibited good performance for glucose detection in an alkaline medium. The linear range was from 0.1×10^{-6} M to 2.2×10^{-3} M with a LOD of 60×10^{-9} M. Similar results were obtained by Archana et al., who prepared a CuO/NiO-C nanocomposite derived from a bimetallic Cu/Ni-based MOF by thermal annealing at 430°C under N_2 atmosphere (Figure 9c).^[113] The CuO/NiO-C composites showed even a lower LOD (37 nm) with a sensitivity of $586.7 \mu\text{A cm}^{-2}/\times 10^{-3}$ M. This improved performance can be attributed to the existence of abundant channels into the composites, which improved both the adsorption and diffusion of glucose on the catalytic sites. A variety of other MO's nanocomposites derived from MOF^[112,113,122–131,114,132–141,115,142–145,116–121] were developed for glucose sensing and Table 3 summarized their composition and relevant analytical performance.

5. MOF-Based Enzymatic Electrochemical Glucose Sensors

MOFs have also been explored for the development of enzymatic electrochemical glucose sensors. Although enzyme-based

sensors have certain restrictions as described in the introduction section, they are more accurate and commercially available for self-monitoring and POC testing applications. However, one of the main challenges of enzyme-based glucose sensors is the difficulty of GO_x immobilization without compromising the electrochemical response.^[1] Several articles report on strategies for the immobilization of GO_x in MOFs, their derivatives and MOF composites without compromising the sensitivity of the sensors. For example, Patra et al. reported a Pt NPs and Fe-MOF (iron(III) trimesate or MIL-100(Fe)) nanocomposite (Figure 10a), which effectively incorporated GO_x .^[58] A suspension of MIL-100(Fe) and GO_x was successively deposited onto an electrodeposited Pt NPs-modified carbon ink electrode (CIE) and then employed for the detection of glucose. Noteworthy is the circumstance that the detection was performed in acetate buffer medium (pH 5.3), i.e., under acidic conditions. Even under these conditions the sensor showed a sensitivity of $71 \text{ mA cm}^{-2} \text{ m}^{-1}$ and a low LOD of 5×10^{-6} M. The good performance can be ascribed to the synergistic effect of Pt NPs and MIL-100(Fe) as well as the high porous structure of MIL-100(Fe), which improved the trapping and the immobilization efficiency of GO_x . In Ref.,^[57] Paul et al. employed a similar strategy to prepare an Au NPs encapsulated ZIF-8 for a mediator-free enzymatic glucose sensor (Figure 10b). This sensing system was able to detect glucose down to nanomolar concentration levels (i.e., 50×10^{-9} M). Other strategies of immobilization of GO_x made use of Zr(IV)-MOF/ionic liquids (IL),^[146] ZIF-8 biocomposites,^[147] Au NPs/Cu-BTC/macroporous carbon,^[148] Cu-hemin MOFs,^[149] Tb@MOFs-CNTs,^[150] and nanoporous carbon derived from Al-PCPs,^[151] which provided a good analytical performance for glucose detection as summarized in Table 4.

MOFs were also used as a peroxidase-like biomimetic catalyst for H_2O_2 reduction to accelerate the GO_x catalyzed glucose oxidation. Wang et al. developed a polydopamine (PDA)/ZIF-8/rGO composite-modified GCE for the detection of glucose, where PDA acted as an immobilization matrix for GO_x and rGO served as the electron transporting channel (Figure 10c).^[61] The H_2O_2 , generated by the GO_x -catalyzed oxidation of glucose to gluconic acid, was reduced to H_2O , mediated by the oxidized form of ZIF-8. The sensor performance provided a linear range from 1×10^{-6} M to 3.6×10^{-3} M, sensitivity of $15\,191 \mu\text{A}/\times 10^{-3}$ M, and LOD of 0.333×10^{-6} M.

6. Optical Glucose Sensors Based on MOFs

Optical transduction-based glucose sensors are beneficial for direct, label-free, and real-time detection within 1–5 min.^[10,11] To date, a large number of optical transduction methods have been developed for glucose sensing, including near-IR spectroscopy, min-IR spectroscopy, CM, Raman spectroscopy, FL, coherence tomography, SPR, optical coherence tomography, Fourier transform near-infrared spectroscopy, and SERS.^[1,152,153] MOFs and their composite-based optical glucose sensors, categorized as enzymatic and nonenzymatic similar to the electrochemical glucose sensors, have been developed based on the CM, FL, chemiluminescence (CL), SERS, and SPR detection methods.^[154–158] In the following section we discuss the principles of CM and FL for glucose

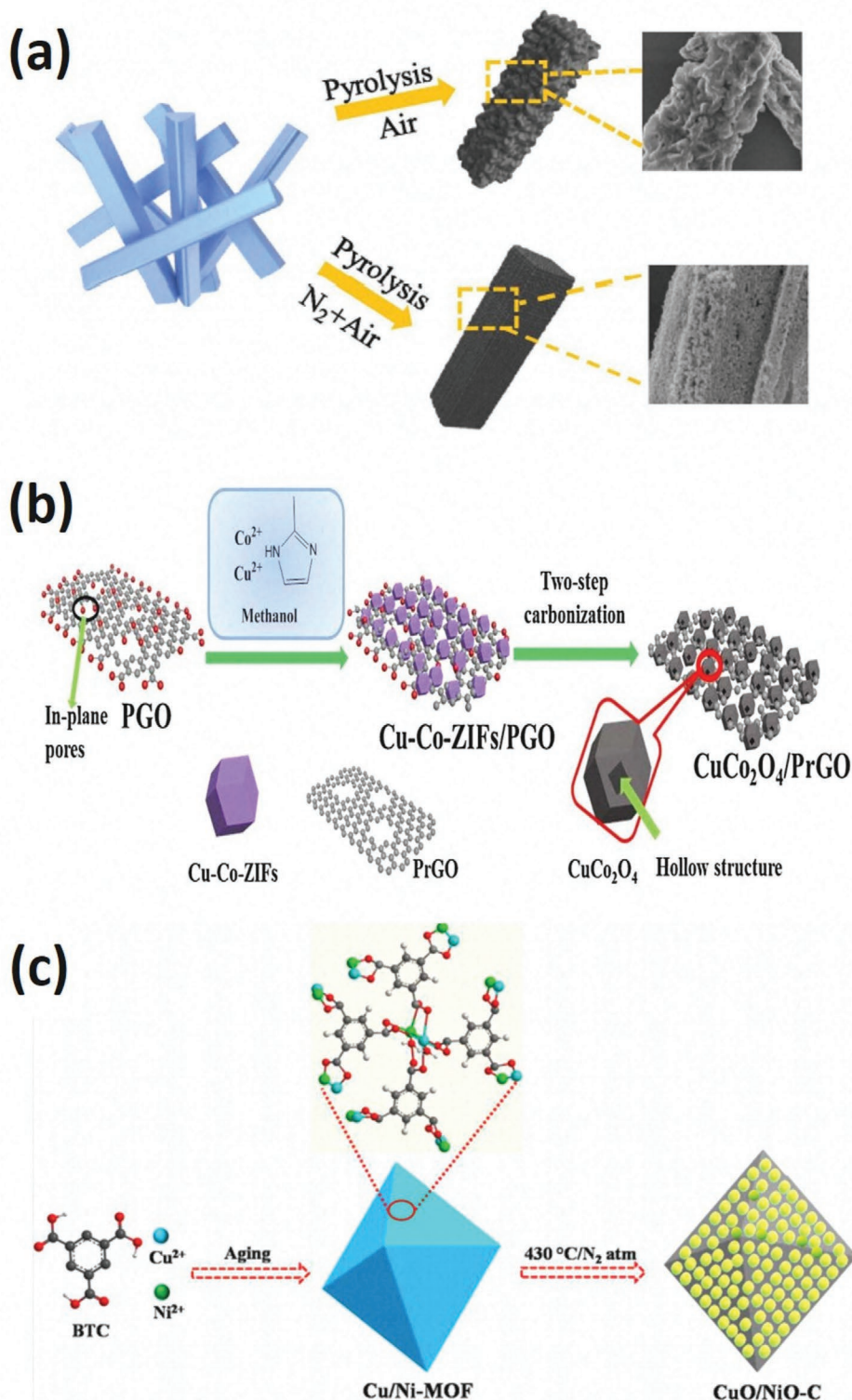


Figure 9. a) Schematic of the synthesis of CuO derived from Cu-MOF and the corresponding SEM images. Reproduced with permission.^[111] Copyright 2020, Royal Society of Chemistry. b) Schematic of the synthesis of MOF-derived CuCo₂O₄/PrGO for glucose oxidation. Reproduced with permission.^[109] Copyright 2017, Elsevier. c) Schematic of the synthesis of MOF-derived CuO/NiO-C composite. Reproduced with permission.^[113] Copyright 2019, American Chemical Society.

Table 3. Analytical performance of nonenzymatic electrochemical glucose sensors based on MOF-derived nanomaterials.

Electrode material	Technique	Linear range [$\times 10^{-6}$ M]	LOD [$\times 10^{-6}$ M]	Sensitivity [$\mu\text{A cm}^{-2}/\times 10^{-6}$ M]	Potential [V]	Ref.
Co@NCD	AMP	0.2–12 000	0.11	125	0.5	[122]
Co(OH) ₂	AMP	5–6700	1.730	-	0.55	[123]
Cu@C ₈₀₀	AMP	200–8000	29.8	0.48 $\mu\text{A}/\times 10^{-3}$ M	0.55	[124]
CuO polyhedrons	AMP	0.5–800	0.46	13 575	0.55	[125]
Nanoporous C/Co ₃ O ₄	DPV	5×10^{-6} – 2.06×10^{-2}	2×10^{-6}	0.14 $\mu\text{A cm}^{-2}/\times 10^{-12}$ M	–	[126]
Cu–Cu ₂ O–CuO/C	CV	up to 1000	–	–	–	[127]
Amorphous Co ₃ O ₄	AMP	0.5–956.5	3.9	1074.22	0.58	[128]
Co NP/Porous C	AMP	100–1100	5.69	227	0.5	[129]
CuO nanorod	CA	up to 1250	1	1523.5	0.6	[130]
Porous CuO	AMP	0.5–2800	0.1	934.2	0.55	[131]
Cu ₂ O@Co ₃ O ₄ core–shell NW	AMP	0.1–1300	0.036	27 778	–	[114]
Fe ₃ O ₄	DPV	0–9000	15.70	4.67	–	[132]
Ni/C	AMP	24–1200	7.87	9.11	0.5	[133]
Cu@ Porous C	AMP	0.15–5620	0.48	28.67	0.45	[134]
CuO	AMP	0.5–5000	0.07	–	0.42	[135]
Co ₃ O ₄	AMP	5–1175	0.2	700	0.58	[136]
Co ₃ O ₄ /CNTs	AMP	5–2000	0.35	22 210	0.55	[137]
NiCo NSs/graphene nanoribbons	AMP	5–800 and 1000–10 000	0.6	344	0.6	[138]
NiCo ₂ O ₄ microflowers	–	1–7800	0.48	–	–	[139]
Co ₃ O ₄ /rGO	AMP	1–500	0.4	1315	0.35	[140]
CoO-Co-NC-rGO	AMP	0.5–10	0.34	3172	0.6	[141]
Cu@ Ni microsphere	AMP	0–5000	0.4	496 $\mu\text{A}/\times 10^{-3}$ M	0.54	[115]
Co ₃ O ₄ /CuO NWs	AMP	0.5–100	0.23	6.0 $\mu\text{A}/\times 10^{-3}$ M	0.5	[142]
3D CuCo-Oxide	AMP	0.05–3300	0.026	41 020	0.55	[143]
ZnO-NiO	AMP	13–4860	4.12	448.6	0.5	[144]
Ni ₃ N@C	AMP	1–3000 and 3–7	0.3	1511.59 and 783.75	0.60	[145]
NiO superstructures	AMP	18–1200	6.15	395 $\mu\text{A}/\times 10^{-3}$ M	0.55	[116]
CuNi/C NS	AMP	200–2720	0.066	17 120	0.54	[117]
Co nanobeads/rGO	AMP	150–6250	47.5	39.32	0.55	[118]
Ni ₂ P/GN	AMP	5–1400	0.44	7234	0.5	[119]
Cu@porous C	AMP	1- 6000	0.6	10 100	0.55	[120]
Ni@C NS	AMP	0.15–1480	0.05	32 790	0.54	[121]

sensing, based on MOFs, MOFs composites, and MOF-derived materials.

6.1. Principles of Detection

The principles of glucose detection based on CM and FL methods are highlighted, as most of the MOFs sensors available in the literature are based on the latter transduction modes (see Table 5).

CM methods possess technical advantages over other optical detection methods such as visual ability and low-cost.^[157] The principles of detection of the enzymatic detection of glucose based on MOF is schematized in Figure 11a. In a GO_x immobilized or

entrapped onto/in MOFs, glucose is enzymatically catalyzed to gluconic acid and H₂O₂. Subsequently, the generated H₂O₂ is reduced by the MOFs due to their peroxidase-like activity. This prompts a characteristic chromogenic reaction in the presence of colored reagents. This color change is a function of the concentration of glucose and it is monitored at a given wavelength.

The FL detection of glucose based on MOFs can be performed by nonenzymatic or enzymatic approaches. In nonenzymatic FL detection systems, fluorescence MOFs act as molecular recognition compounds or fluorophores.^[159] Upon glucose binding or entrapped into the pores of MOFs, a change in the fluorescence signal occurs. The change in the FL intensity is proportional to the concentration of glucose (Figure 11b).

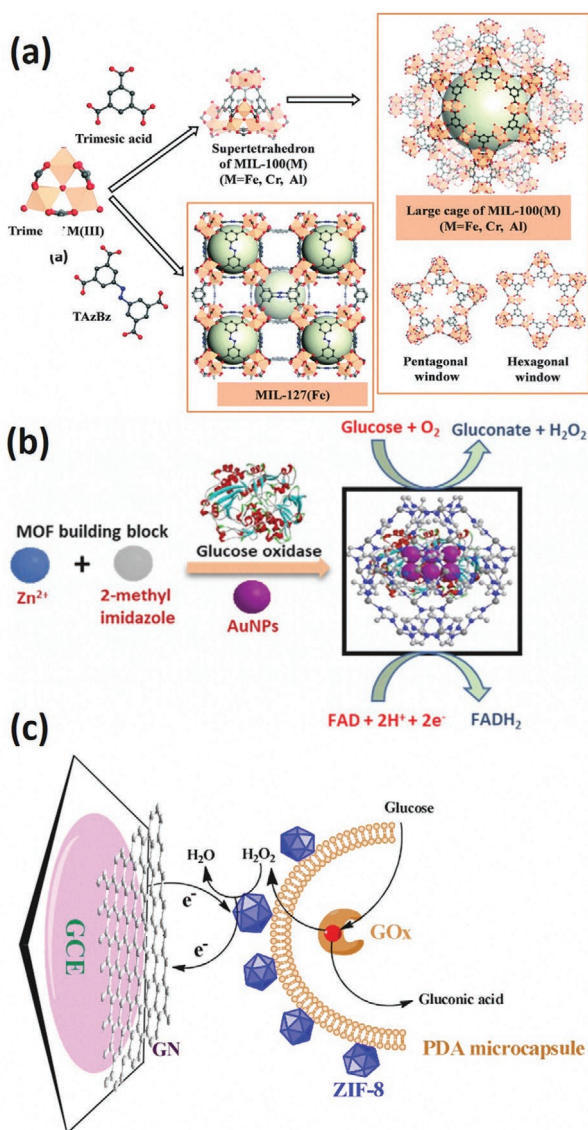


Figure 10. a) Schematic illustration of the synthesis of MIL-100 (M) for glucose oxidation. Reproduced with permission.^[60] Copyright 2015, Royal Society of Chemistry. b) Schematic illustration of the preparation of GO_x and Au NPs encapsulated ZIF-8 composites for glucose oxidation. Reproduced with permission.^[57] Copyright 2018, American Chemical Society. c) Schematic of the reaction mechanism of glucose oxidation and H₂O₂ reduction at the GO_x/PDA/ZIF-8/rGO sensors. Reproduced with permission.^[61] Copyright 2016, Royal Society of Chemistry.

The mechanism of the enzymatic FL glucose sensor is similar to the enzyme-based CM sensors (Figure 11c). In this case, a fluorescent probe is used in place of color reagents.^[156] Upon excitation at a certain wavelength, the fluorescent probe emits light, whose intensity is proportional to the concentration of glucose.

6.2. Enzymatic Glucose Sensors

The literature reports a variety of enzymatic MOFs based glucose sensors, exploiting optical transduction approaches. For

example, Xu et al. immobilized GO_x onto an -NH₂ functionalized MOFs (Fe-MIL-88B-NH₂) via a covalent interaction by post-modification method (Figure 12a).^[160] The remarkable peroxidase-like activity of Fe-MIL-88B-NH₂ and the catalytic activity of GO_x for the oxidation of glucose enabled cascade catalysis for the CM detection of glucose at pH 4.0 by the oxidation of color reagent tetramethylbenzidine (TMB). The analytical characteristics were linear range from 1×10^{-6} to 500×10^{-6} M and LOD of 0.487×10^{-6} M. In Ref.,^[157] Zhao et al. developed a similar CM detection method of glucose at pH 4.0, based on the GO_x@ZIF-8@Fe-PDA hybrid shell. In this case, GO_x was embedded in ZIF-8 by the co-precipitation approach (Figure 12b). The peroxidase mimicking of the ZIF-8@Fe-PDA hybrid shell and the GO_x induced oxidation of glucose, followed by a cascade catalytic reaction for the CM detection of glucose by the oxidation of TMB. The linear range was 5.0×10^{-6} – 100.0×10^{-6} M and LOD of 1.1×10^{-6} M. A similar co-precipitation method was applied for the preparation of GO_x-Fe(III)-BTC by Zhao et al.^[161] The Fe(III)-BTC acted as a peroxidase mimicking and solid support for the immobilization of GO_x (Figure 12c). Again, GO_x-Fe(III)-BTC enabled glucose oxidation by a cascade catalysis reaction. The linear range and LOD were 5.0×10^{-6} – 100×10^{-6} M and 2.4×10^{-6} M, respectively. Based on similar cascade catalytic reactions, other researchers developed Fe(III)porphyrin-MOF,^[162] MIL-53(Fe),^[163] glycine functionalized MIL-53(Fe),^[164] and hemin/MIL-101(Al)-NH₂ hybrid^[165] for the immobilization or entrapment of GO_x and the subsequent CM detection.

In a FL-based enzymatic glucose sensor, as mentioned above, a fluorescent probe is used. It is oxidized by H₂O₂ upon the cascade reactions induced by the oxidation of glucose to gluconic acid. Shi et al. developed a 2D Cu-MOF (Cu(bpy)₂(OTf)₂) for the entrapment of GO_x by post-synthetic method (Figure 13a).^[156] The cascade oxidation reaction of glucose to gluconic acid catalyzed by GO_x and the subsequent reduction of H₂O₂ catalyzed by Cu-MOF induced the formation of the highly fluorescent thiochrome from the nonfluorescent thiamine. The analytical method revealed to be highly selective with two linear ranges, specifically over 0.01×10^{-3} – 0.1×10^{-3} M and 0.1×10^{-3} – 1×10^{-3} M, and a LOD of 0.41×10^{-6} M. In another report, Lin et al. prepared a GO_x enzyme-modified peroxidase mimicking MIL-53(Fe) for FL detection of glucose. The linker terephthalic acid (TA) in MIL-53(Fe) served as the fluorescent probe (Figure 13b).^[166] The cascade reactions, involving the oxidation and reduction of glucose and H₂O₂, respectively, induced the formation of the fluorescent hydroxylated TA, from the nonfluorescent TA, thus facilitating the detection of glucose with good analytical performance.

In a CL transduction-based enzymatic detection of glucose, luminol is used as a CL probe, which is oxidized and generates strong CL signals upon the cascade reaction induced by glucose oxidation to gluconic acid and the subsequent reduction of H₂O₂.^[167,184,185] The CL intensity of the oxidized luminol is directly proportional to the concentration of glucose. Zhu et al. developed a CL glucose sensor based on a 2D MOF (Co-TCPP(Fe)).^[155] The peroxidase activity of Co-TCPP(Fe) reduced the H₂O₂ generated by the oxidation of glucose and oxidized luminol, thus providing strong CL signals. The sensor was able to detect glucose in urine samples with good sensitivity ($10.667 \mu\text{g L}^{-1}$) in a wide concentration range (32 – $5500 \mu\text{g L}^{-1}$). Tang et al. synthesized a Fe₃O₄/MIL-101(Fe) composite, a peroxidase-like enzyme, which at the

Table 4. Analytical performance of enzymatic electrochemical glucose sensors based on MOFs, MOFs composites, and MOF derived materials.

Electrode material	Detection Method	Linear range [$\times 10^{-6}$ M]	LOD [$\times 10^{-6}$ M]	Sensitivity [$\mu\text{A cm}^{-2}/\times 10^{-3}$ M]	Ref.
Zr(IV)-MOF/IL	AMP	8–100 and 100–2000	2.7	$1.9 \mu\text{A}/\times 10^{-3}$ M	[146]
GO _x /ZIF-8 bio-composites	AMP	0–7500	2.2	1.88	[147]
AuNPs/Cu-BTC/C	DPV	44.9–4000 and 4000–19 000	14.77	–	[148]
Cu-hemin MOFs	LSV	9.10–36 000	2.73	22.77	[149]
Tb@MOFs-CNTs	CV	25–17 000	8	–	[150]
Nanoporous carbon derived from Al-PCPs	CV	70–990	65	$6.81 \mu\text{A}/\times 10^{-3}$ M	[151]

end of the cascade reactions, induced by GO_x, led to the oxidation of luminol (Figure 13c).^[183] The GO_x and luminol were mixed with Fe₃O₄/MIL-101(Fe) composite. This system was able to detect glucose over the concentration range from 5×10^{-9} to 100×10^{-9} M, with a LOD of 4.9×10^{-9} .

Similar cascade reactions strategies were exploited to construct other enzymatic glucose sensors based on MOFs and their subclasses (In-MOF, MIL-53(Fe), Fe-MIL-88NH₂, MIL-101(Fe), magnetic ZIF-8, ZIF-8 (NiPd), MIL-53(Fe), and ZIF-8),^[159,166–172] MOF composites (AuNPs@MIL-101(Cr), Au@MIL-100(Fe), Hemin@MIL-53(Al)-NH₂, Cu-hemin MOFs, Cu-MOF/Fe₃O₄-AuNPs, AuNPs@ Cu-TCPP, Ficin@Zn-MOF, Ag NPs-porphyrin MOF, Cu(II)/Co(II) organic gel, g-C₃N₄@Cu-MOF,

and hemin@HKUST-1 MOF),^[154,158,165,173–180] and MOF derived materials (CoNPs/C and Cu@C-500)^[181,182] using CM, FL, CL, SERS, and SPR transduction methods, which are included in Table 5, together with the corresponding analytical performance.

6.3. Nonenzymatic Glucose Sensors

There are only a few examples reported in the literature concerning the use of MOFs for the enzymeless detection of glucose exploiting optical transduction approaches. This is conceivably related to the poor selectivity of chemical events, compared to that of an enzymatic reaction. Kumar et al. developed a

Table 5. Analytical performance of reported CM, FL, CL, SERS, and SPR transduction systems of enzymatic glucose sensors based on MOFs, MOF composites, and MOF-derived materials.

Materials	Detection method	Reagents/Probe	Linear range [$\times 10^{-6}$ M]	LOD [$\times 10^{-6}$ M]	Ref.
Pristine MOFs					
In-MOF	FL	In-MOF	0–160	0.87	[159]
MIL-53(Fe)	FL	TAOH	0.5–27	0.0084	[166]
Fe-MIL-88NH ₂	CM	TMB	2–300	0.48	[167]
MIL-101(Fe)	CM	TMB	100–1000	0.4	[168]
Magnetic ZIF-8	CM	OPD	5–150	1.9	[169]
ZIF-8 (NiPd)	CM	OPD	10–300	9.2	[170]
MIL-53(Fe)	CL	Luminol	0.1–10	0.05	[171]
ZIF-8	Wave guide	–	1000–8000	–	[172]
MOF composite					
AuNPs@MIL-101(Cr)	SERS	–	10–200	4.2	[154]
Au@MIL-100(Fe)	SPR	–	0–12 000	–	[158]
Hemin@MIL-53(Al)-NH ₂	CM	TMB	10–300	–	[165]
Cu-hemin MOFs	CM	TMB	10–300	6.9	[173]
Cu-MOF/Fe ₃ O ₄ -AuNPs	CM	TMB	12.86–257.14	12.20	[174]
AuNPs@ Cu-TCPP	CM	TMB	1–300	8.5	[175]
Ficin@Zn-MOF	CM	TMB	1–140	0.12	[176]
Ag NPs-Porphyrin MOF	FL	Ag NPs	5–80	0.078	[177]
Cu(II)/Co(II) organic gel	FL	TA	0.5–120	0.33	[178]
g-C ₃ N ₄ @Cu-MOF	FL	TA	0.1–22	0.059	[179]
Hemin@HKUST-1 MOF	CL	Luminol	7.5–75	7.5	[180]
MOF derived materials					
CoNPs/C	CL	TMB	0.25–30	0.156	[181]
Cu@C-500	CM	TMB	50–350	0.32	[182]

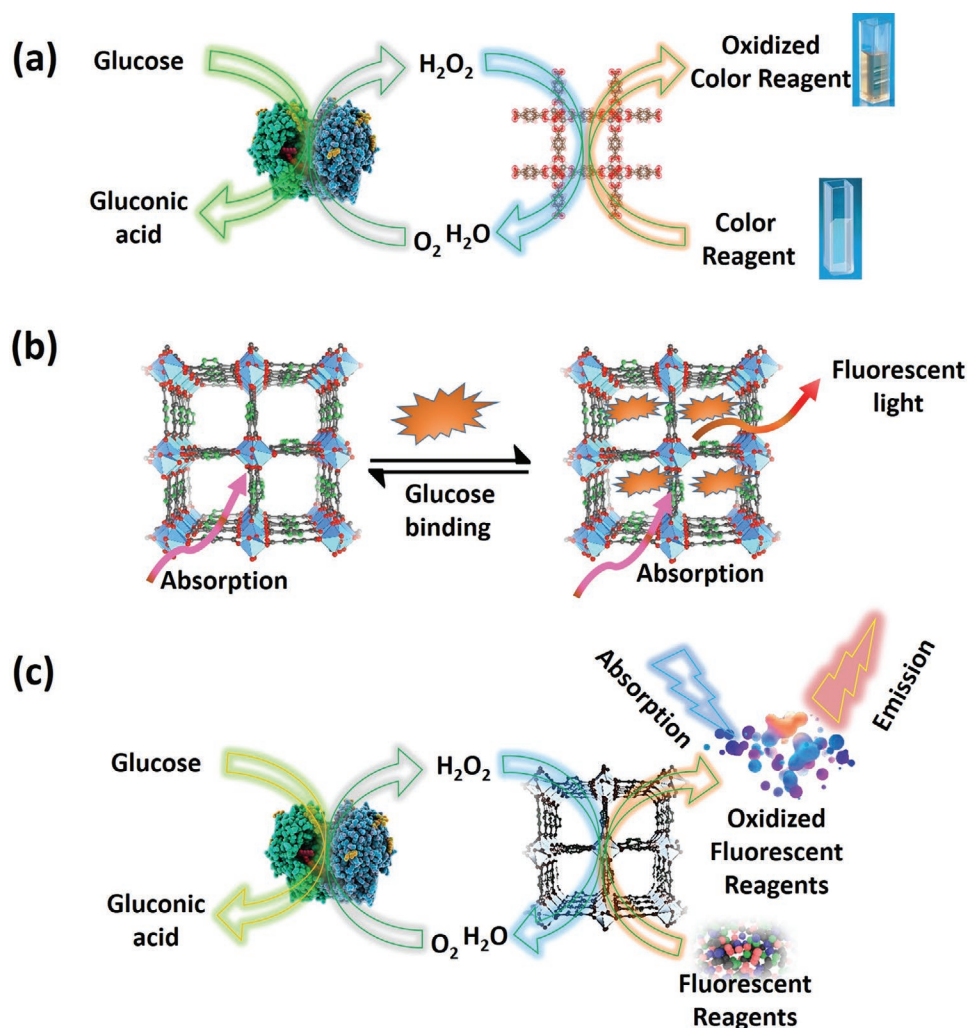


Figure 11. Schematic of the general principles of MOFs-based a) enzymatic CM, b) nonenzymatic FL, and c) enzymatic FL glucose detection system.

FL sensor using a Zn-based MOF (IRMOF-3) having an average size of 160 ± 20 nm and synthesized by a simple hydrothermal method. This material showed strong emission and absorption peaks at 460 nm and 355 nm, respectively.^[186] The $-\text{NH}_2$ and $-\text{COOH}$ functional groups present on the MOF surface allowed binding of the cis-diols of the glucose molecule via host-guest interaction. This led to a remarkable quenching in the fluorescence intensity of the MOF. The FL intensity of IRMOF-3 decreased linearly with the logarithmic concentration of glucose in the range from 1×10^{-6} to 225×10^{-6} M, providing a LOD of 0.56×10^{-6} M. Despite the host-guest interaction that could exert to some extent selectivity toward glucose, the authors do not provide any information on interference due to other biological molecules.

Hu et al. developed AuNPs and porphyrin-based MOFs composites (AuNPs/Cu-TCPP(Fe)) for the detection of glucose by exploiting a SERS-transduction method.^[187] The AuNPs/Cu-TCPP(Fe) hybrid was prepared by in situ modification of AuNPs onto the Cu-TCPP(Fe). The authors claimed that AuNPs mimicked the GO_x like properties, while Cu-TCPP(Fe) acted as a peroxidase mimicking. Thus, the cascade catalysis reactions

occurred, as those described above for the GO_x -based sensors, and H_2O_2 induced the oxidation of non-Raman-active leucomalachite green into the Raman-active malachite green. The hybrid material enabled glucose detection in the concentration range from 0.16×10^{-3} to 8×10^{-3} M with a LOD of 3.9×10^{-6} M.

7. MOF-Based Wearable and Flexible Glucose Sensors

Traditional blood glucose meters measure the blood glucose concentration invasively. To overcome this limitation and to extend the possibility of glucose monitoring noninvasively during, for instance, physical exercise or work, flexible and wearable devices have been developed.^[188] Wearable and flexible sensors are easy to integrate into clothes, contact lenses, watch, and rings for continuous glucose measurements in sweat, tears, and saliva. The glucose concentrations in the latter body fluids are statistically related to the blood glucose concentration.^[1,7] Therefore, the detection of glucose can be performed noninvasively by using wearable sensors. Human sweat contains glucose concentration

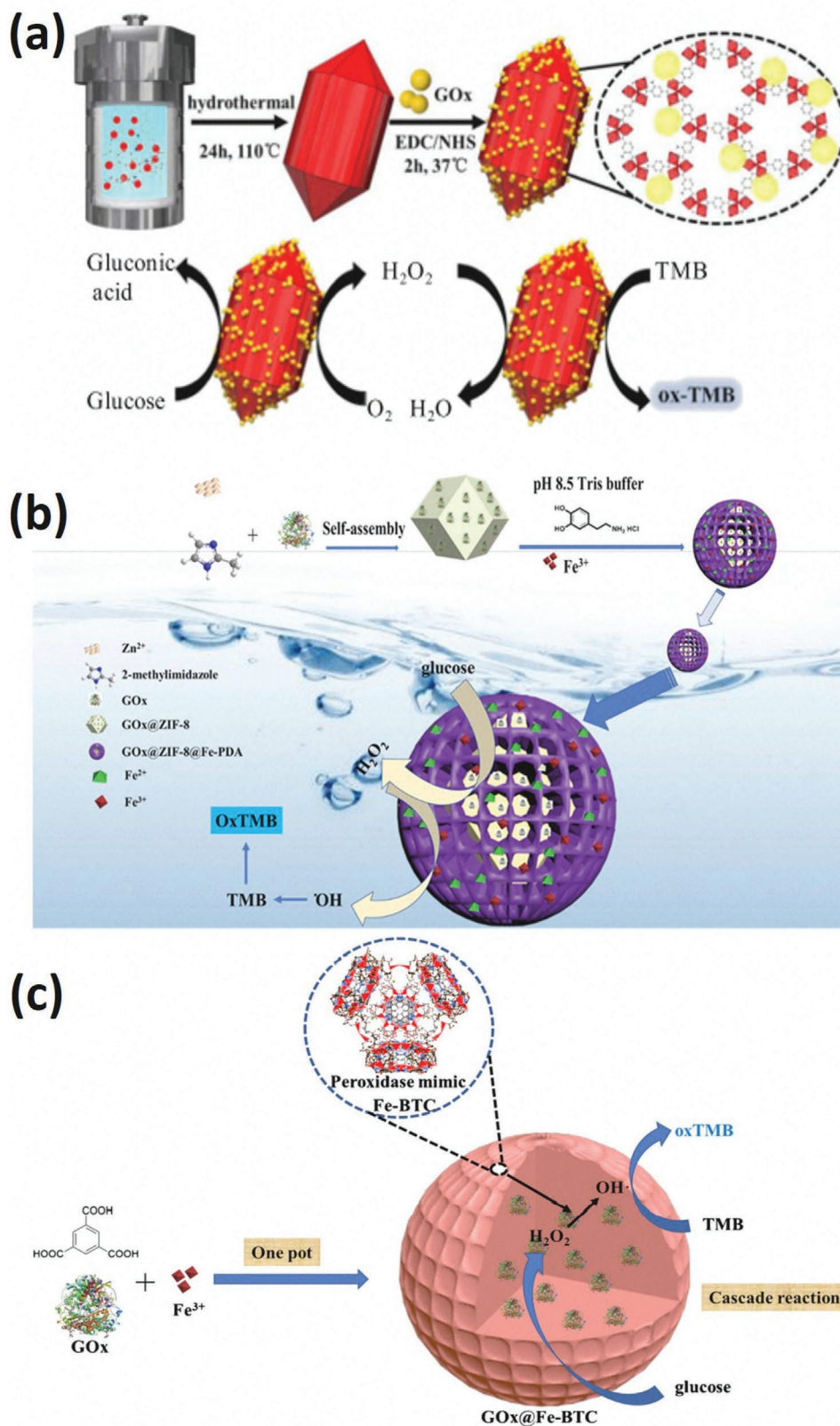


Figure 12. a) Schematic illustration of the synthesis Fe-MIL-88B-NH₂-GO_x and the reaction mechanism for the cascade oxidation of glucose. Reproduced with permission.^[160] Copyright 2019, American Chemical Society. b) Schematic illustration of the synthesis of GO_x@ZIF-8@Fe-PDA hybrid shell and the reaction mechanism for the cascade oxidation of glucose. Reproduced with permission.^[157] Copyright 2019, Elsevier. c) Schematic illustration of the synthesis of GO_x-Fe(III)-BTC and the reaction mechanism for glucose oxidation. Reproduced with permission.^[161] Copyright 2019, Springer.

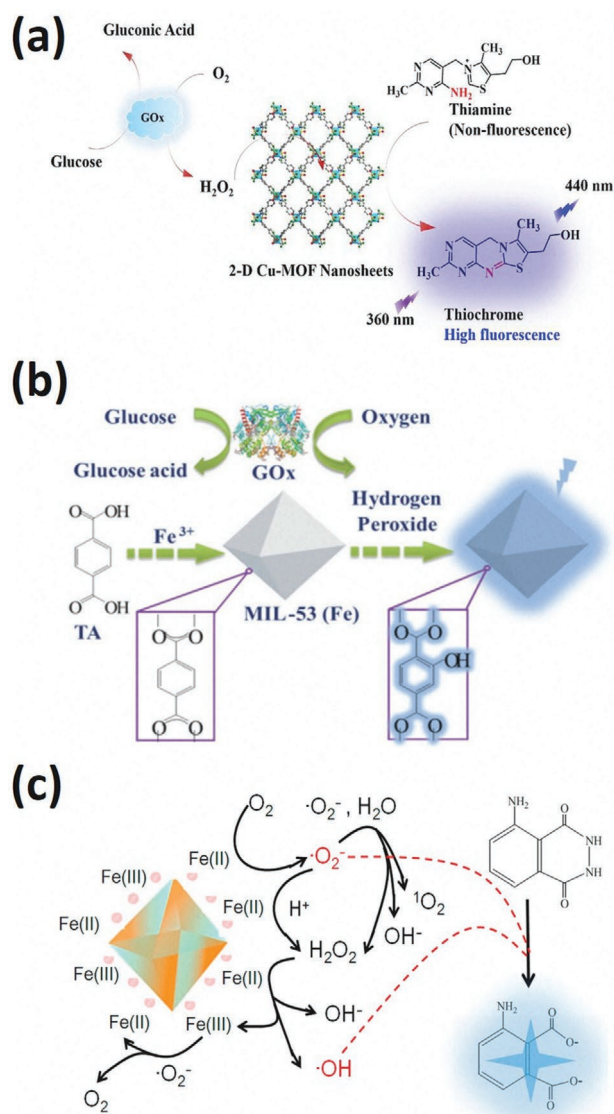


Figure 13. a) Schematic of the reaction mechanism of FL detection of glucose based on a Cu-MOF. Reproduced with permission.^[156] Copyright 2019, Elsevier. b) Schematic of the reaction mechanism of FL detection of glucose based on MIL-53(Fe). Reproduced with permission.^[166] Copyright 2018, Royal Society of Chemistry. c) Plausible reaction mechanism for $\text{Fe}_3\text{O}_4/\text{MIL-101(Fe)}$ catalyze luminol CL. Reproduced with permission.^[183] Copyright 2018, Elsevier.

in the range from 5.6×10^{-6} to 2200×10^{-6} M, while it is ca. 0.92×10^{-3} M in the tears of diabetic patients.^[189,190] Most of the MOFs-based glucose sensors available in the literature fulfill the latter analytical requirements. In the following sections, we summarize the recent progress and developments of wearable and flexible electrochemical and optical glucose sensors based on MOFs, MOF composites, and MOF-derived materials.

7.1. Electrochemical

Enzymatic and nonenzymatic wearable and flexible glucose sensors were developed exploiting the intrinsic nanozyme

activity or the high and tuneable porosity of MOFs that allow immobilizing or entrapping GO_x in their structures. Zhu et al. developed a flexible and wearable nonenzymatic glucose sensor based on Pd NPs encapsulated ZIF-67 (Pd@ZIF-67), which can detect glucose at physiological pH without any additional reagents (Figure 14a).^[191] The sensor was integrated into a wearable sweatband for real-time glucose monitoring in sweat and were transmitted using a smartphone. The system was very stable and sensitive for up to two months under ambient conditions, working over a concentration range varying from 10×10^{-6} to 1000×10^{-6} M. In another article, Xuan et al. developed a flexible carbon fiber electrode modified with a Ni-MOF for the enzymeless electrochemical detection of glucose in sweat (Figure 14b).^[192] The as-prepared Ni-MOF exhibited longitudinal expansion leading to an increase of the number of active sites of Ni ions, which enhanced the sensitivity of glucose detection. This Ni-MOF-based flexible sensor with a PVA/NaOH solid-state electrolyte was employed to detect glucose in sweat in the concentration range from 0 to 1600×10^{-6} M with a sensitivity of $470.40 \mu\text{A cm}^{-2}/\times 10^{-3}$ M. Another flexible platform was developed by Wei et al. by depositing conducting leaflike Co-MOF onto a flexible carbon cloth (CC) for the electrocatalytic oxidation of glucose in an alkaline medium. The analytical characteristics of the sensor were: linear range from 0.004×10^{-3} to 4.428×10^{-3} M, sensitivity of $1113 \mu\text{A cm}^{-2}/\times 10^{-3}$ M, and LOD of 1.2×10^{-6} M.^[193] This sensor was applied to detect glucose just in human blood serum. Some other researchers developed flexible and enzymeless electrochemical detection systems of glucose, based on a variety of MOFs composites, including CuO/NiO/carbon nanocomposites deposited on cello tape,^[113] sandpaper-supported Cu-MOF,^[194] Co-MOF/CC/paper,^[195] ZIF-67/carbon fibers,^[196] Cu-catecholate (Cu-CAT) MOF fractals/carbon paper,^[197] and Cu-Co-ZIF derivatives/CC.^[198] The analytical performances of these sensors are summarized in Table 6, which indicated that the bimetallic 2D Cu-Co-ZIF derivative modified flexible CC electrode showed remarkably high sensitivity compared to the reported other pristine MOFs, MOF composites, and MOF-derived materials,^[198] conceivably due to the enriched reaction sites induced by the 2D structures as well as the synergistic effect of $\text{Cu}^{1+/2+}$ and $\text{Co}^{2+/3+}$ redox pairs formed in an alkaline medium for the mediated oxidation of glucose. Most of these flexible MOFs-based sensors were, however, applied to more common body fluids such as human blood serum, urine, saliva.

Enzyme-based flexible glucose sensors based on MOFs have also been developed. Li et al. prepared a GO_x encapsulated ZIF-8 on a cellulose acetate nanofiber membrane as a highly flexible electrode for glucose detection.^[199] The in-situ encapsulation of GO_x into ZIF-8 improved the stability of the ZIF-8@ $\text{GO}_x/\text{MWCNTs}/\text{Au}$ sensor up to 15 h for continuous glucose monitoring. The linear range was from 1×10^{-3} to 10×10^{-3} M and a LOD of 5.347×10^{-6} M. The sensor promises easy integration into a wearable device for glucose monitoring in human sweat at the physiological state (Figure 14c). Similarly, Co-MOF modified PET plastic substrate^[200] and Au NPs/ZIF-8 modified plastic chip^[201] were developed as the enzymatic and flexible platforms for glucose detection and relevant analytical performance are shown in Table 6. Noteworthy, the Co-MOF modified PET plastic substrate was employed for in vivo interstitial fluids

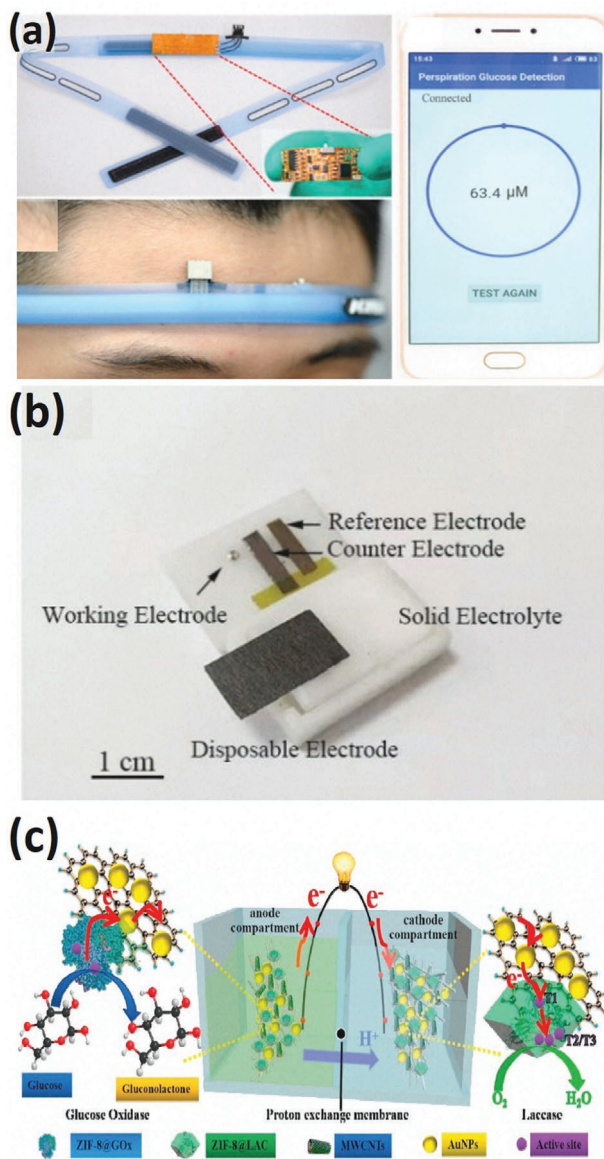


Figure 14. a) Wearable and smartphone-assisted glucose monitoring system in sweat based on Pd@ZIF-67 with the corresponding analytical performance. (Reproduced with permission.^[191] Copyright 2019, American Chemical Society. b) Digital photograph of Ni-MOF/carbon fiber-based all-solid-state enzymeless sweat glucose sensor. Reproduced with permission.^[192] Copyright 2020, Royal Society of Chemistry. c) Schematic illustration of the GO_x/ZIF-8 modified cellulose acetate nanofiber membrane-based self-powered glucose biosensor. Reproduced with permission.^[199] Copyright 2021, Elsevier.

measurement. To this purpose, the sensor was inserted into the abdominal cavity of anesthetized mouse and the glucose amount was recorded for about 5 min.

7.2. Optical

The optical transduction-based wearable and flexible glucose sensors have been investigated limitedly due to their high cost and the difficulty of miniaturization. Additionally, optical wearable and flexible glucose sensors need complex fabrication steps, costly optical fibers, and spectrophotometers coupled to a computer. Therefore, wearable optical sensors are not mass-produced for POC testing of glucose. Nevertheless, in the literature, some examples of wearable optical sensors based on MOFs exist. This section summarizes MOF-based flexible and in vivo optical platforms for glucose detection.

Huang et al. prepared an Ag@Au nano prisms-Ir-Zn_e MOF composite to modify a flexible paper electrode for enzymatic detection of glucose in human serum and urine by a luminescence method (Figure 15a).^[202] The Ag@Au nanoprisms were deposited into a paper substrate; subsequently, the phosphorescent luminophores Ir-Zn_e MOF was superimposed on Ag@Au nanoprisms. This composite significantly enhanced the emission intensity of the MOFs due to the coupling of the MOF dipoles with the localized SPR band of Ag@Au nanoprisms. Upon the addition of glucose, O₂ molecules are consumed by the oxidation of glucose, resulting in the enhancement of the phosphorescence intensity of the MOF. This enabled the detection of glucose with a fast response time (5 s), over the concentration range of 0.05 × 10⁻³–30 × 10⁻³ M; a LOD of 0.038 × 10⁻³ M was calculated. In another report, Cheng et al. developed an enzymatic CM sensor based on an integrated nanozymes (INAzymes) by simultaneously embedding hemin and GO_x inside ZIF-8 (GO_x/hemin@ZIF-8) (Figure 15b,c).^[203] The cascade reaction induced by the oxidation of glucose catalyzed by GO_x and the reduction of H₂O₂ by the peroxidase mimicking hemin@ZIF-8 enabled the oxidation of the colored substrate ABTS. The catalytic activity of this INAzyme enabled in vivo analysis of cerebral glucose in the concentration range from 0 to 250 × 10⁻⁶ M. A LOD of 1.7 × 10⁻⁶ M calculated.

8. MOF-Based Field-Effect Transistors Devices for Glucose Sensing

Transistors are semiconductor devices used to amplify the signal and switch circuits. There are two main types of

Table 6. Analytical performance of flexible electrochemical glucose sensors based on MOFs, MOF-composite, and MOF-derived materials.

Electrode material	Substrate	Linear range [× 10 ⁻⁶ M]	LOD [× 10 ⁻⁶ M]	Sensitivity [μA cm ⁻² /× 10 ⁻³ M]	Ref.
Co-MOF	CC/paper	800–16 000	150	–	[195]
ZIF-67	Carbon fibers	0.5–30	0.3	4835	[196]
Cu-Co-ZIF derivatives	CC	20–800	2	18 680	[198]
Co-MOF	PET	–	54.6	–	[200]
Au NPs/ZIF-8	Plastic chip	–	0.06	–	[201]

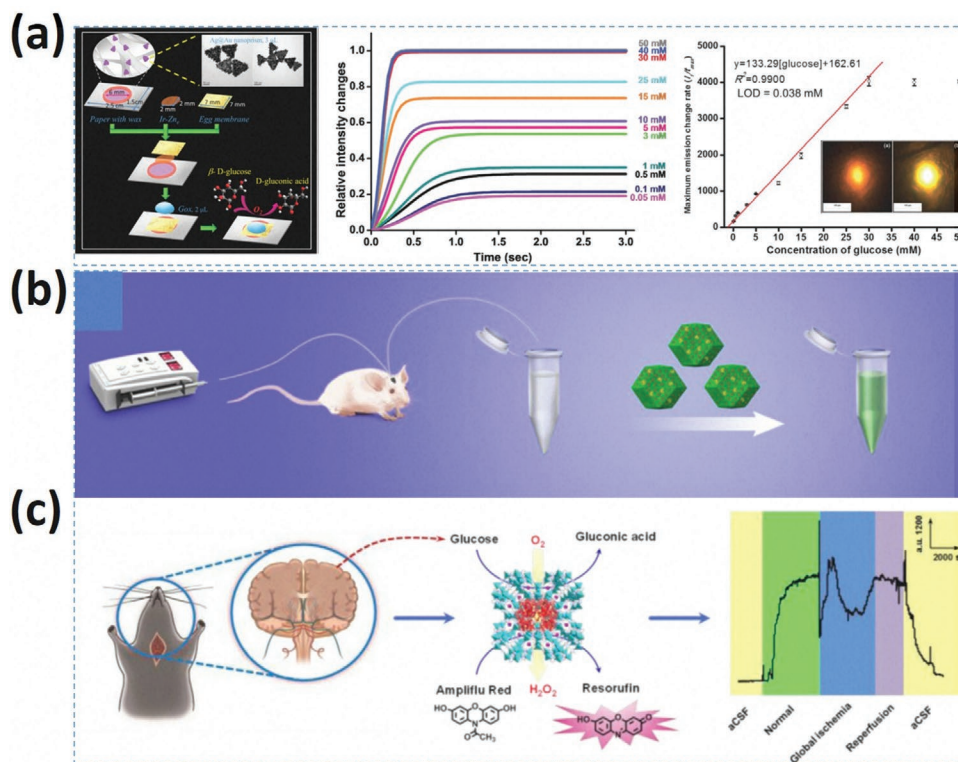


Figure 15. a) Fabrication process and sensing mechanism of Ag@Au nano prisms- Ir-Zn₆ MOF modified flexible paper sensor and the corresponding luminescence intensity variation with the variation of glucose concentrations and calibration curve. Reproduced with permission.^[202] Copyright 2017, Royal Society of Chemistry. b,c) Schematic illustration of glucose monitoring in the brain of living rates based on INAzyme, and the schematic illustration of the integrated system along with cascade reactions mechanism for the detection of glucose in living brain. Reproduced with permission.^[203] Copyright 2016, American Chemical Society.

transistors: Field-effect (FET) and bipolar junction.^[204] FET-based biosensors or “bio-FET” are attractive for label-free and real-time monitoring of a variety of target molecules. In addition, they are easy to use and cost-effective.^[204,205] In a typical FET system, the target analytes bind to the sensing channels leading to the change of the source-drain “channel” conductivity. The electrical conductivity or resistance at the channel is inversely proportional to the carrier density, which is measured from a change in the source-drain voltage-current characteristics.^[205] The channel conductance varies as a function of the concentration of the target molecules. A large number of FET devices based on various nanomaterials for sensing different biomolecules, including proteins, nucleotides, and glucose, have been developed.^[206–208] MOF materials have been investigated to develop FET-based glucose sensors, albeit to a limited extent. This is due to the low conductivity of MOFs and the difficulty of their integration into the channel with good contact and intactness.^[209] Nevertheless, a few examples FET-based glucose sensors, using MOFs and their derivatives, have been developed and their main characteristics are briefly described below.

Wang et al. developed an enzymatic FET glucose sensor based on a bimetallic Ni/Cu-MOF as channel layers (Figure 16a).^[210] The Ni/Cu-MOF film was grown uniformly onto the channel of pre-prepared FET devices and then modified with GO_x by using glutaraldehyde (GA) as linkers. The sensor operation involves the catalytic oxidation of glucose by GO_x with the production of

H₂O₂. Under the applied gate voltage, H₂O₂ oxidises and generates H⁺ and e⁻. The amount of H⁺ formed by the continuous enzymatic reaction accumulates at the interface between p-type Ni/Cu-MOF channel layers and the solution. The holes formed in the Ni/Cu-MOFs channel film react with H⁺, resulting in a decrease of the current value of the FET, proportionally to glucose concentration. This sensor provides a linear range from 0.001×10^{-3} to 20×10^{-3} M, a sensitivity of $26.05 \mu\text{A cm}^{-2}/\times 10^{-3}$ M, and a LOD of 0.51×10^{-6} M.

In order to improve the electrical conductivity of the channels of FET, MOF-derived materials, containing carbon composites appeared highly suitable. Inspired by this, Xiong et al. synthesized a concave-shaped N-doped carbon framework embedded with single site Co (Co SSC) derived from Cobalt phthalocyanine@ZIF-8 by pyrolysis (Figure 16b,c).^[211] The as-prepared Co SSC was mixed with GO_x and used to modify the Au gate electrode of a solution-gated graphene transistor (SGGT). This Co SSC-based SGGT significantly improved the sensitivity of glucose detection of three orders of magnitude with respect to the device produced without the catalyst. This allowed achieving a LOD down to 10×10^{-9} . In another report, Xiong et al. developed a ZIF-67 derived porous Co₃O₄ hollow nanopolyhedron to prepare GO_x-CS/Co₃O₄ composites (Figure 16d).^[212] The as-prepared GO_x-CS/Co₃O₄ was used to modify the Au gate electrode of SGGT for glucose detection. The working operation of the sensor involved the cascade reactions, described in previous

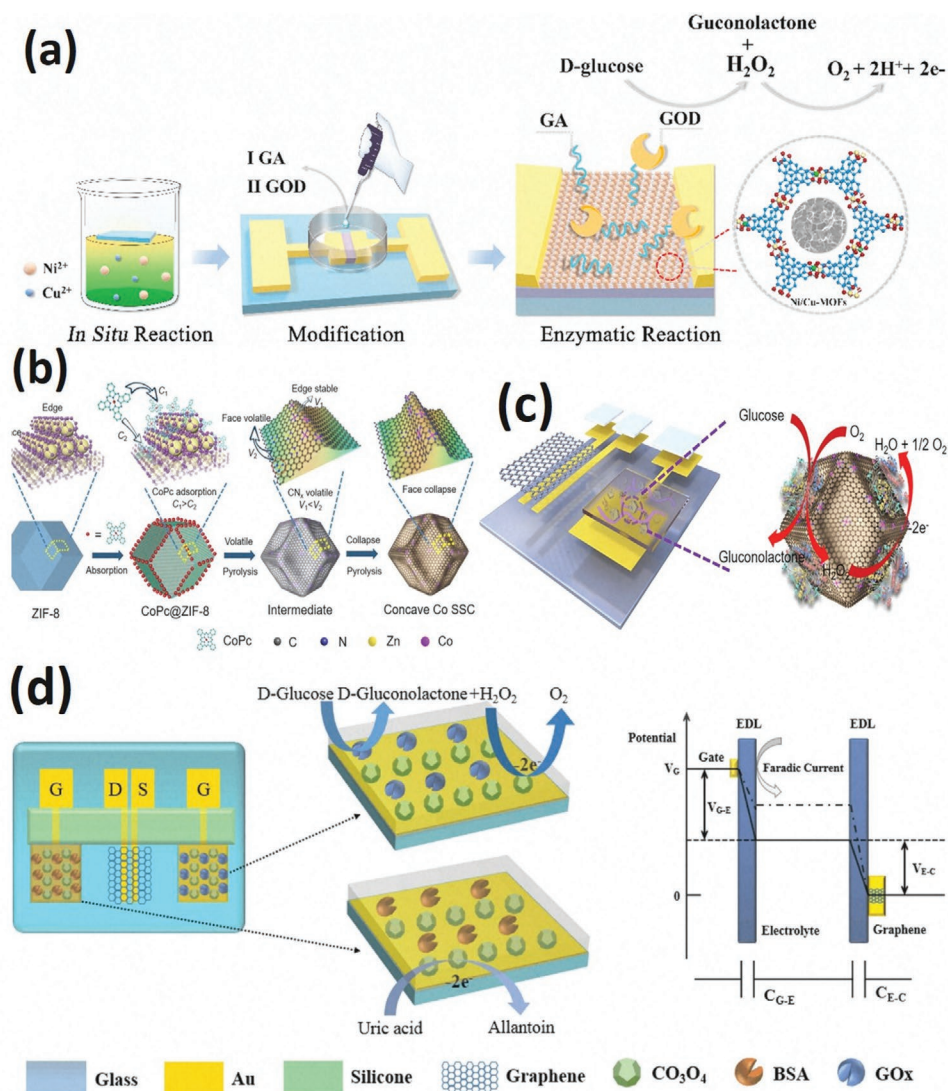


Figure 16. a) Schematic of the synthesis process and sensing mechanism of $\text{GO}_x\text{-GA-Ni}/\text{Cu-MOFs}$ -based FET for glucose detection. Reproduced with permission.^[210] Copyright 2021, Elsevier. b,c) Schematic of the synthesis processes of Co SSC and sensing mechanism of $\text{GO}_x\text{-Co SSC}$ based SGGT for glucose detection. Reproduced with permission.^[211] Copyright 2020, Elsevier. d) Schematic diagram of a $\text{GO}_x\text{-CS}/\text{Co}_3\text{O}_4/\text{Au}$ gate electrode-based SGGT and sensing mechanism. Reproduced with permission.^[212] Copyright 2018, Elsevier.

sections, induced by the glucose oxidation by GO_x , the formation of H_2O_2 , which reacts near the gate and changes the channel current, and consequently a change of the gate voltage proportionally to the glucose concentration. Again, the sensitivity of the modified sensor was improved to such an extent to provide a LOD down to 100×10^{-9} , which was 1000-fold lower than that found with the unmodified Au gate electrode. These sensors were employed to detect glucose in tears.

9. MOF-Based Microfluidic Devices for Glucose Sensing

Microfluidic is the science and technology that appeared in the early 1980s and denotes the precise control and manipulation of small amounts of fluids using channels with dimensions

at the microscale levels (tens to hundreds of micrometers).^[213] Until now, microfluidic has been applied in multi-disciplinary fields, including biology and medicine,^[214–219] chemistry,^[220–224] surface chemistry,^[225,226] electrochemistry,^[223,224,227] and micro-technology^[226,228] with the advantages of the consumption of small sample volume (10^{-9} – 10^{-18} liters). Microfluidic technology has been rationalized for about two decades, offering the advantage of low cost, short assay time, high specificity, low power consumption, reduced waste production, high sensitivity, and multiple target detection. Consequently, a lot of microfluidic biosensors have been developed, including DNA-, enzymes-, and immunoassay-based microfluidics biosensors.^[229–231] Initially, conventional soft lithography was used to make a microfluidic channel for continuous flow regimes. Later, this technology has been replaced with droplet-based microfluidic devices that are useful to reduce the sample consumptions and segregation of reaction sites. Even

smaller consumption of sample volume has been achieved by the introduction of the digital microfluidic systems. In these devices, sample droplets are created on the array of electrostatically active electrodes rather than as laminar flow of samples.^[232]

A microfluidic sensing platform is generally composed of a recognition element and a transducing device, similar to other biosensor systems. The commonly used transduction methods in a microfluidic sensor are optical, electrochemical, and impedimetric.^[233] The recognition elements (e.g., enzymes, antibodies, ssDNA, etc.) in an affinity biosensor bind the target analyte, whereas, for catalytic biosensors, the recognition element induces a chemical reaction or electron transfer. To obtain high sensitivity, reproducibility, and stability, the immobilization or entrapment of recognition elements into the microfluidic channel is crucial, and it can be attained by modifying the channels with various types of affinity-based and catalytically active nanomaterials. The immobilization or entrapment of GO_x with high surface coverage into the microfluidic channel enabled by nanomaterials significantly enhanced the sensitivity of glucose detection. In particular, pristine or functionalized MOFs are attractive materials to improve the immobilization or entrapment of GO_x . This section summarized recent developments of MOF-based microfluidic systems for the detection of glucose.

Ilacas et al. reported a paper-based microfluidic (μ PADs) sensor for enzymatic detection of glucose using $\text{GO}_x@Zr\text{-PCN-222(Fe)-MOF}$ via CM method without the use of coloring agents (Figure 17a,b).^[43] The $\text{GO}_x@Zr\text{-PCN-222(Fe)}$ was used to prepare two different configurations of μ PADs, i.e., well-based and lateral flow assay (LFA). For well-based μ PADs, $\text{GO}_x@Zr\text{-PCN-222(Fe)}$ was spotted between the chip layers, followed by the assembly of the platform. A solution of KI and glucose was spotted into the well, inducing a yellow-brown color spot in the μ PADs. In the LFA-based μ PADs, the chips were sandwiched between parafilm layers and further sandwiched between PVA layers. $\text{GO}_x@Zr\text{-PCN-222(Fe)}$ was spotted onto the inlet, allowing it to flow laterally into the outlet, followed by the addition of glucose with varying concentrations. This yielded a yellow-brown color that enabled glucose detection. Similarly, Gómez et al. developed a μ PAD for glucose sensing using $\text{GO}_x/\text{Fe-MIL-101}$ via CM method and TMB as coloring agent (Figure 17c).^[234] The Fe-MIL-101 presented a peroxidase-like activity for the reduction of H_2O_2 produced by the enzymatic oxidation of glucose. The subsequent oxidation of TMB, induced by the reduction of H_2O_2 , generated a green-blue color that was revealed by a digital camera. The method employed allowed the achievement of a LOD of 2.5×10^{-6} M. Other researchers developed $\text{GO}_x/\text{hemin@ZIF-8}$ ^[203] and $\text{ZIF-8}/\text{GO}_x\&\text{HRP}$ ^[235]-based microfluidic devices for glucose detection with good analytical results and stability.

10. Conclusions, Challenges, and Future Outlooks

This review highlighted the advances of MOFs, their subtypes, MOF composites, and MOF-derived materials for the

construction of electrochemical, optical, FET, and microfluidic device for the detection of glucose. Both nonenzymatic and enzymatic detection systems also as flexible and wearable devices have been described. The review also deals with the design and synthesis of MOFs to develop the various types of sensors and the fundamental mechanisms of the different transduction methods involved in glucose detection.

In general, MOFs and their derivatives showed high catalytic activity for electrochemical enzymeless glucose detection in alkaline medium, similar to other nanozymes (e.g., MO and their composites). These properties arise from the redox activity of Mn^+ /cluster Mn^+ of the MOFs in an alkaline medium, which mediated the oxidation of glucose. Thus, one of the main challenges of MOF-based electrochemical enzymeless sensing is the development of redox-active materials able to work at physiological pH, allowing glucose detection in biological fluids and avoiding the time-consuming sample treatments. One possible way to achieve this result is by controlling the size, inherent chemical properties, and general structures of MOFs, as reported in a recent paper concerning a 2D MAF-5- Co^{II} material.^[24] Another aspect to be considered is the poor chemical stability and the low conductivity of MOFs. This drawback can be resolved by preparing MOFs using hydrophobic linkers, chemically inert or low labile Mn^+ , multi Mn^+ , post-modification, insertion of size-matching ligands as brackets into the pores, post-synthetic exchange via metal-ion metathesis, post-synthetic modifications with long-alkyl substituents, and hydrophobic surface treatment.

In contrast, an enzymatic glucose sensor based on the physical entrapment of GO_x into the pores of MOFs can catalyze glucose oxidation at physiological pH. The reliability of enzymatic glucose sensors is still a huge concern, because of the well-known and the above extensively discussed instability of GO_x . Moreover, the physical entrapment of large dimensional GO_x into the pores of MOFs cannot guarantee the reproducibility and reliability of the sensor. Fortunately, many different free guest-accessible functional groups (e.g., $-\text{NH}_2$, $-\text{SO}_3\text{H}$, $-\text{NO}_2$, $-\text{NHCO}-$, and $-\text{NHCONH}-$) contained MOFs have already been developed, and GO_x can be immobilized onto/into these functional MOFs by chemical interaction with strong binding to obtain high stability of enzyme-based sensors.

Optical transduction-based glucose detection systems are highly reliable and accurate for CGM though they are costly and difficult to miniaturize. MOFs and their derivative-based optical glucose sensors are mainly based on GO_x enzyme, using CM, FL, and CL detection methods. Along with limitations due to the GO_x stability and physical entrapment onto/into MOFs, optical sensors fabrication is complex and requires coloured/fluorescent probes. Some specific MOFs, exhibiting peroxidase-like activity, are used for the CM, FL, and CL-based detection of glucose via cascade type reactions. Because, commonly used coloured or fluorescent probes are organic dyes, they display photobleaching and toxicity effects. To overcome these drawbacks, a future direction for the CM and FL-based glucose sensors is the development of MOFs with eco-friendly organic linkers, which can also act as fluorescent probes. As for nonenzymatic optical glucose detection systems based on MOFs and their derivatives, they have

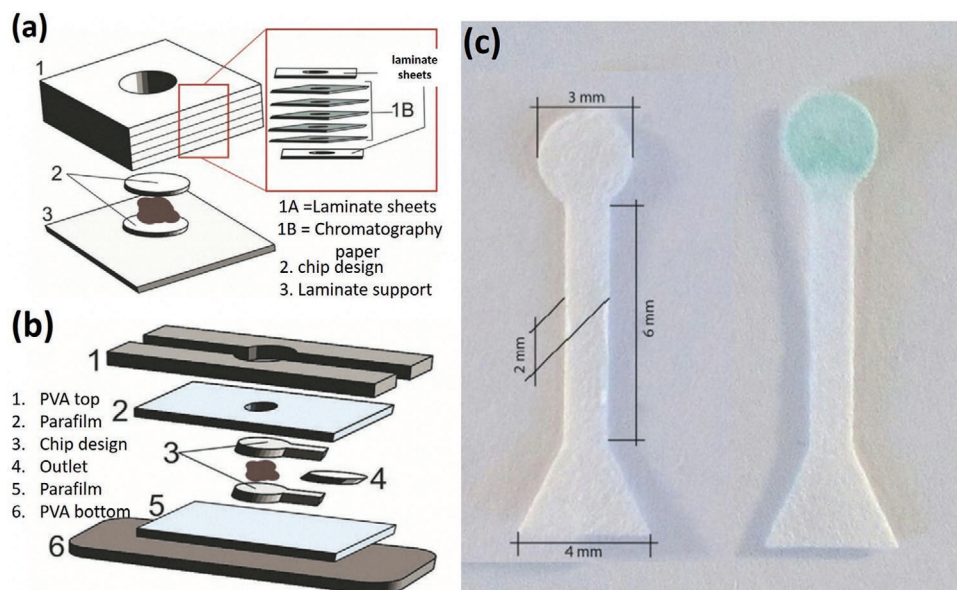


Figure 17. Schematic illustration of a) well-based μ PAD and b) LFA-based μ PAD constructed using $\text{GO}_x/\text{Zr-PCN-222}(\text{Fe})\text{-MOF}$. Reproduced with permission.^[43] Copyright 2019, Elsevier. c) Digital photographs of $\text{GO}_x/\text{Fe-MIL-101}$ based μ PAD before and after reaction with glucose. Reproduced with permission.^[234] Copyright 2017, Springer.

been much less investigated, mainly due to the weak luminescence properties of MOFs themselves. The post-modification of MOFs, by incorporating suitable luminescent guests or luminophores inside the pores or backbone, can represent an effective strategy to develop nonenzymatic optical glucose sensors. Also, controlling the size and dimension of MOFs can effectively tune their luminescence properties.

FET-based devices are advantageous over optical detection systems and comparable to electrochemical systems. The main challenge in the development of a high-performance MOFs-based FET device is the low conductivity and difficulty of MOFs integration into the channel with good contact and intactness. Development of MOFs composite using highly conductive nanoscale materials and functional MOFs for chemical immobilization of GO_x can be the effective strategy to minimize the limitations due to the low conductivity and weak binding of GO_x . The main drawback of FET-based systems for biomolecules detection, including glucose, is the limitation arising from the “Debye screening length” or the shielding generated by the electrical double layer. This can be overcome by preparing ultrathin arrays of MOFs and their derivatives into the FET channels.

A microfluidic device for glucose detection is advantageous over other current detection methods due to its low cost and durability. Microfluidic is an attractive area of research and development due to the increasing demand for biomedical devices and chips to detect multianalyte. So far, MOFs are used to develop enzyme-based microfluidic devices with the CM detection method. The main drawbacks of this system are related to the fabrication processes, photobleaching, and toxic coloring reagents. These limitations can be overcome by the development of electrochemical and impedimetric microfluidic devices based on MOFs. This can also open the road toward the transformation of the microfluidic sensor technology from bench to POC and point-of-need diagnosis of glucose.

Finally, during the preparation of this review, we felt that MOFs, MOF composites, and MOF-derived materials for glucose detection are advancing at an unparalleled rate. After about two decades since the first introduction in the late 1990s,^[236] MOF is finding its place for nonenzymatic catalytic glucose oxidation and also as GO_x immobilization matrix for enzymatic glucose detection. The first examples of these possibilities appeared in the literature only in 2002. Thus, sooner we might observe the first large-scale and commercial applications of MOFs after resolving the critical chemical instability, redox inactivity at neutral pH, and low conductivity issues of the materials.

Acknowledgements

This work was financially supported by SPIN—Supporting Principal Investigators, Ca’ Foscari University of Venice, Italy. The authors are sorry for all the authors that work in this field and were not cited in this manuscript due to the space limitation.

Conflict of Interest

The authors declare no conflict of interest.

Keywords

electrochemical devices, enzymatic sensors, field-effect transistors, glucose sensors, metal–organic frameworks, microfluidics, nonenzymatic, optical sensors

Received: June 23, 2021
Revised: August 26, 2021
Published online:

- [1] M. Adeel, M. M. Rahman, I. Caligiuri, V. Canzonieri, F. Rizzolio, S. Daniele, *Biosens. Bioelectron.* **2020**, *165*, 112331.
- [2] J. Hippisley-Cox, C. Coupland, *BMJ* **2016**, *352*, 24.
- [3] P. Saeedi, I. Petersohn, P. Salpea, B. Malanda, S. Karuranga, N. Unwin, S. Colagiuri, L. Guariguata, A. A. Motala, K. Ogurtsova, J. E. Shaw, D. Bright, R. Williams, *Diabetes Res. Clin. Pract.* **2019**, *157*, 107843.
- [4] International Diabetes Foundation, International Diabetes Federation—Facts & Figures, <https://idf.org/aboutdiabetes/what-is-diabetes/facts-figures.html> (accessed: May 2021).
- [5] American Diabetes Association, Diagnosis and Classification of Diabetes Mellitus, *Diabetes Care* **2009**, *32*, S62.
- [6] X. Strakosias, J. Selberg, P. Pansodtee, N. Yonas, P. Manapongpun, M. Teodorescu, M. Rolandi, *Sci. Rep.* **2019**, *9*, 10844.
- [7] H. Teymourian, A. Barfidokht, J. Wang, *Chem. Soc. Rev.* **2020**, *49*, 7671.
- [8] A. Heller, B. Feldman, *Chem. Rev.* **2008**, *108*, 2482.
- [9] I. L. Jernelv, K. Milenko, S. S. Fuglerud, D. R. Hjelm, R. Ellingsen, A. Aksnes, *Appl. Spectrosc. Rev.* **2019**, *54*, 543.
- [10] W. V. Gonzales, A. T. Mobashsher, A. Abbosh, *Sensors* **2019**, *19*, 800.
- [11] N. S. Oliver, C. Toumazou, A. E. G. Cass, D. G. Johnston, *Diabetic Med.* **2009**, *26*, 197.
- [12] M. Grady, M. Pineau, M. K. Pynes, L. B. Katz, B. Ginsberg, *J. Diabetes Sci. Technol.* **2014**, *8*, 691.
- [13] A. Pfützner, C. Schipper, S. Ramljak, F. Flacke, J. Sieber, T. Forst, P. B. Musholt, *J. Diabetes Sci. Technol.* **2013**, *7*, 1522.
- [14] Z. Yared, K. Aljaberi, N. Renouf, J. F. Yale, *Diabetes Care* **2005**, *28*, 1836.
- [15] A. Tura, A. Maran, G. Pacini, *Diabetes Res. Clin. Pract.* **2007**, *77*, 16.
- [16] S. K. Krishnan, E. Singh, P. Singh, M. Meyyappan, H. S. Nalwa, *RSC Adv.* **2019**, *9*, 8778.
- [17] F. Qu, Y. Zhang, A. Rasooly, M. Yang, *Anal. Chem.* **2014**, *86*, 973.
- [18] I. U. Hassan, H. Salim, G. A. Naikoo, T. Awan, R. A. Dar, F. Arshad, M. A. Tabidi, R. Das, W. Ahmed, A. M. Asiri, A. H. Qurashi, *J. Saudi Chem. Soc.* **2021**, *25*, 101228.
- [19] M. M. Rahman, A. J. S. Ahammad, J. H. Jin, S. J. Ahn, J. J. Lee, *Sensors* **2010**, *10*, 4855.
- [20] S. Y. Tee, C. P. Teng, E. Ye, *Mater. Sci. Eng., C* **2017**, *70*, 1018.
- [21] X. Yan, Y. Gu, C. Li, B. Zheng, Y. Li, T. Zhang, Z. Zhang, M. Yang, *Anal. Methods* **2018**, *10*, 381.
- [22] G. R. Xu, C. Ge, D. Liu, L. Jin, Y. C. Li, T. H. Zhang, M. M. Rahman, X. B. Li, W. Kim, *J. Electroanal. Chem.* **2019**, *847*, 113177.
- [23] M. T. Ulhakim, M. Rezki, K. K. Dewi, S. A. Abrori, S. Harimurti, N. L. W. Septiani, K. A. Kurnia, W. Setyaningsih, N. Darmawan, B. Yuliarto, *J. Electrochem. Soc.* **2020**, *167*, 136509.
- [24] M. Adeel, V. Canzonieri, S. Daniele, A. Vomiero, F. Rizzolio, M. M. Rahman, *Microchim. Acta* **2021**, *188*, 77.
- [25] N. S. Lopa, M. M. Rahman, F. Ahmed, T. Ryu, J. Lei, I. Choi, D. H. Kim, Y. H. Lee, W. Kim, *J. Electroanal. Chem.* **2019**, *840*, 263.
- [26] B. G. Amin, J. Masud, M. Nath, *J. Mater. Chem. B* **2019**, *7*, 2338.
- [27] D. Branagan, C. B. Breslin, *Sens. Actuators, B* **2019**, *282*, 490.
- [28] D. W. Hwang, S. Lee, M. Seo, T. D. Chung, *Anal. Chim. Acta* **2018**, *1033*, 1.
- [29] M. Elsherif, M. U. Hassan, A. K. Yetisen, H. Butt, *ACS Nano* **2018**, *12*, 5452.
- [30] M. Bajgrowicz-Cieslak, Y. Alqurashi, M. I. Elshereif, A. K. Yetisen, M. U. Hassan, H. Butt, *RSC Adv.* **2017**, *7*, 53916.
- [31] Z. Yu, N. Jiang, S. G. Kazarian, S. Tasoglu, A. K. Yetisen, *Prog. Biomed. Eng.* **2021**, *3*, 022004.
- [32] P. K. Bharadwaj, P. Feng, S. Kaskel, Q. Xu, *Chem. Asian J.* **2019**, *14*, 3450.
- [33] S. K. Yadav, G. K. Grandhi, D. P. Dubal, J. C. de Mello, M. Otyepka, R. Zbořil, R. A. Fischer, K. Jayaramulu, *Small* **2020**, *16*, 2004891.
- [34] H. V. Doan, H. Amer Hamzah, P. Karikkethu Prabhakaran, C. Petrillo, V. P. Ting, *Nano-Micro Lett.* **2019**, *11*, 54.
- [35] S. Sundriyal, H. Kaur, S. K. Bhardwaj, S. Mishra, K. H. Kim, A. Deep, *Coord. Chem. Rev.* **2018**, *369*, 15.
- [36] Z. Wang, H. Tao, Y. Yue, *ChemElectroChem* **2019**, *6*, 5358.
- [37] C. H. Chuang, C. W. Kung, *Electroanalysis* **2020**, *32*, 1885.
- [38] Q. Wang, D. Astruc, *Chem. Rev.* **2020**, *120*, 1438.
- [39] M. Zhao, Y. Huang, Y. Peng, Z. Huang, Q. Ma, H. Zhang, *Chem. Soc. Rev.* **2018**, *47*, 6267.
- [40] H. Beitollahi, Q. Van Le, O. K. Farha, M. Shokouhimehr, S. Tajik, F. G. Nejad, K. O. Kirlikovali, H. W. Jang, R. S. Varma, *Cryst. Growth Des.* **2020**, *20*, 7034.
- [41] Y. S. Wei, M. Zhang, R. Zou, Q. Xu, *Chem. Rev.* **2020**, *120*, 12089.
- [42] Y. H. Budnikova, *Dalton Trans.* **2020**, *49*, 12483.
- [43] G. C. Ilacas, A. Basa, K. J. Nelms, J. D. Sosa, Y. Liu, F. A. Gomez, *Anal. Chim. Acta* **2019**, *1055*, 74.
- [44] I. Stassen, N. Burtch, A. Talin, P. Falcaro, M. Allendorf, R. Ameloot, *Chem. Soc. Rev.* **2017**, *46*, 3185.
- [45] S. Carrasco, *Biosensors* **2018**, *8*, 92.
- [46] Y. Z. Chen, R. Zhang, L. Jiao, H. L. Jiang, *Coord. Chem. Rev.* **2018**, *362*, 1.
- [47] B. N. Bhadra, A. Vinu, C. Serre, S. H. Jung, *Mater. Today* **2019**, *25*, 88.
- [48] N. Stock, S. Biswas, *Chem. Rev.* **2012**, *112*, 933.
- [49] A. Karmakar, A. V. Desai, S. K. Ghosh, *Coord. Chem. Rev.* **2016**, *307*, 313.
- [50] S. Yuan, L. Zou, J. S. Qin, J. Li, L. Huang, L. Feng, X. Wang, M. Bosch, A. Alsalmeh, T. Cagin, H. C. Zhou, *Nat. Commun.* **2017**, *8*, 15356.
- [51] H. V. Doan, A. Sartbaeva, J. C. Eloi, S. A. Davis, V. P. Ting, *Sci. Rep.* **2019**, *9*, 10887.
- [52] N. S. Lopa, M. M. Rahman, F. Ahmed, S. Chandra Sutradhar, T. Ryu, W. Kim, *Electrochim. Acta* **2018**, *274*, 49.
- [53] M. Ding, X. Cai, H. L. Jiang, *Chem. Sci.* **2019**, *10*, 10209.
- [54] S. M. Cohen, *Chem. Rev.* **2012**, *112*, 970.
- [55] C. Chen, Q. Xie, D. Yang, H. Xiao, Y. Fu, Y. Tan, S. Yao, *RSC Adv.* **2013**, *3*, 4473.
- [56] H. Lee, Y. J. Hong, S. Baik, T. Hyeon, D. H. Kim, *Adv. Healthcare Mater.* **2018**, *7*, 1701150.
- [57] A. Paul, G. Vyas, P. Paul, D. N. Srivastava, *ACS Appl. Nano Mater.* **2018**, *1*, 3600.
- [58] S. Patra, T. Hidalgo Crespo, A. Permyakova, C. Sicard, C. Serre, A. Chaussé, N. Steunou, L. Legrand, *J. Mater. Chem. B* **2015**, *3*, 8983.
- [59] S. Libertino, V. Aiello, A. Scandurra, M. Renis, F. Sinatra, *Sensors* **2008**, *8*, 5637.
- [60] A. Karmakar, A. J. L. Pombeiro, *Coord. Chem. Rev.* **2019**, *395*, 86.
- [61] Y. Wang, C. Hou, Y. Zhang, F. He, M. Liu, X. Li, *J. Mater. Chem. B* **2016**, *4*, 3695.
- [62] D. Zhang, J. Zhang, R. Zhang, H. Shi, Y. Guo, X. Guo, S. Li, B. Yuan, *Talanta* **2015**, *144*, 1176.
- [63] L. Wu, Z. W. Lu, Y. Ma, J. J. Zhang, G. Q. Mo, H. J. Du, J. S. Ye, *Chin. J. Anal. Chem.* **2020**, *48*, 20038.
- [64] Y. Sun, Y. Li, N. Wang, Q. Q. Xu, L. Xu, M. Lin, *Electroanalysis* **2018**, *30*, 474.
- [65] J. Chen, H. Yin, S. Zhao, J. Gong, Z. Ji, Q. Nie, L. Wang, *Funct. Mater. Lett.* **2020**, *13*, 2050022.
- [66] N. S. Lopa, M. M. Rahman, F. Ahmed, S. C. Sutradhar, T. Ryu, W. Kim, *J. Electroanal. Chem.* **2018**, *822*, 43.
- [67] L. Zhang, X. Ma, H. Liang, H. Lin, G. Zhao, *J. Mater. Chem. B* **2019**, *7*, 7006.
- [68] S. Shahrokhian, E. Khaki Sanati, H. Hosseini, *Biosens. Bioelectron.* **2018**, *112*, 100.
- [69] Y. Li, M. Xie, X. Zhang, Q. Liu, D. Lin, C. Xu, F. Xie, X. Sun, *Sens. Actuators, B* **2019**, *278*, 126.

- [70] T. Wang, Y. Yu, H. Tian, J. Hu, *Electroanalysis* **2014**, *26*, 2693.
- [71] A. Benchettara, A. Benchettara, *Mater. Today* **2015**, *2*, 4212.
- [72] K. Okada, S. Sawai, K. Ikigaki, Y. Tokudome, P. Falcaro, M. Takahashi, *CrystEngComm* **2017**, *19*, 4194.
- [73] X. Xiao, S. Zheng, X. Li, G. Zhang, X. Guo, H. Xue, H. Pang, *J. Mater. Chem. B* **2017**, *5*, 5234.
- [74] L. Zhang, N. Wang, P. Cao, M. Lin, L. Xu, H. Ma, *Microchem. J.* **2020**, *159*, 105343.
- [75] J. P. Zhang, Y. B. Zhang, J. Bin Lin, X. M. Chen, *Chem. Rev.* **2012**, *112*, 1001.
- [76] N. Li, J. Xu, R. Feng, T. L. Hu, X. H. Bu, *Chem. Commun.* **2016**, *52*, 8501.
- [77] L. S. Xie, G. Skorupskii, M. Dincă, *Chem. Rev.* **2020**, *120*, 8536.
- [78] X. W. Liu, T. J. Sun, J. L. Hu, S. D. Wang, *J. Mater. Chem. A* **2016**, *4*, 3584.
- [79] J. Yu, C. Mu, B. Yan, X. Qin, C. Shen, H. Xue, H. Pang, *Mater. Horiz.* **2017**, *4*, 557.
- [80] P. Wen, P. Gong, J. Sun, J. Wang, S. Yang, *J. Mater. Chem. A* **2015**, *3*, 13874.
- [81] Z. Wang, J. Huang, J. Mao, Q. Guo, Z. Chen, Y. Lai, *J. Mater. Chem. A* **2020**, *8*, 2934.
- [82] F. X. Qin, S. Y. Jia, Y. Liu, X. Han, H. T. Ren, W. W. Zhang, J. W. Hou, S. H. Wu, *Mater. Lett.* **2013**, *101*, 93.
- [83] E. Doustkhah, R. Hassandoost, A. Khataee, R. Luque, M. H. N. Assadi, *Chem. Soc. Rev.* **2021**, *50*, 2927.
- [84] F. Wang, X. Chen, L. Chen, J. Yang, Q. Wang, *Mater. Sci. Eng., C* **2019**, *96*, 41.
- [85] X. Chen, D. Liu, G. Cao, Y. Tang, C. Wu, *ACS Appl. Mater. Interfaces* **2019**, *11*, 9374.
- [86] X. Zhang, Y. Xu, B. Ye, *J. Alloys Compd.* **2018**, *767*, 651.
- [87] W. Zheng, Y. Liu, P. Yang, Y. Chen, J. Tao, J. Hu, P. Zhao, *J. Electroanal. Chem.* **2020**, *862*, 114018.
- [88] Y. Shu, Y. Yan, J. Chen, Q. Xu, H. Pang, X. Hu, *ACS Appl. Mater. Interfaces* **2017**, *9*, 22342.
- [89] D. Arif, Z. Hussain, M. Sohail, M. A. Liaquat, M. A. Khan, T. Noor, *Front. Chem.* **2020**, *8*, 573510.
- [90] J. Zhang, L. Chen, K. Yang, *Ionics* **2019**, *25*, 4447.
- [91] S. Ranganathan, S.-M. Lee, J. Lee, S.-C. Chang, *J. Sens. Sci. Technol.* **2017**, *26*, 379.
- [92] N. Yang, K. Guo, Y. Zhang, C. Xu, *J. Mater. Chem. B* **2020**, *8*, 2856.
- [93] A. Paul, D. N. Srivastava, *ACS Omega* **2018**, *3*, 14634.
- [94] J. Chen, Q. Xu, Y. Shu, X. Hu, *Talanta* **2018**, *184*, 136.
- [95] L. Xiao, Q. Zhao, L. Jia, Q. Chen, J. Jiang, Q. Yu, *Electrochim. Acta* **2019**, *304*, 456.
- [96] Y. Wen, W. Meng, C. Li, L. Dai, Z. He, L. Wang, M. Li, J. Zhu, *Dalton Trans.* **2018**, *47*, 3872.
- [97] J. Chen, H. Yin, J. Zhou, L. Wang, J. Gong, Z. Ji, Q. Nie, *J. Electron. Mater.* **2020**, *49*, 4754.
- [98] L. Zhang, H. Liang, X. Ma, C. Ye, G. Zhao, *Microchem. J.* **2019**, *146*, 479.
- [99] C. Hou, Q. Xu, L. Yin, X. Hu, *Analyst* **2012**, *137*, 5803.
- [100] H. Zou, D. Tian, C. Lv, S. Wu, G. Lu, Y. Guo, Y. Liu, Y. Yu, K. Ding, *J. Mater. Chem. B* **2020**, *8*, 1008.
- [101] X. Peng, Y. Wan, Y. Wang, T. Liu, P. Zou, X. Wang, Q. Zhao, F. Ding, H. Rao, *Electroanalysis* **2019**, *31*, 2179.
- [102] Y. Zhou, Q. Hu, F. Yu, G. Y. Ran, H. Y. Wang, N. D. Shepherd, D. M. D'Alessandro, M. Kurmoo, J. L. Zuo, *J. Am. Chem. Soc.* **2020**, *142*, 20313.
- [103] G. Zang, W. Hao, X. Li, S. Huang, J. Gan, Z. Luo, Y. Zhang, *Electrochim. Acta* **2018**, *277*, 176.
- [104] W. Meng, Y. Wen, L. Dai, Z. He, L. Wang, *Sens. Actuators, B* **2018**, *260*, 852.
- [105] L. Shi, X. Zhu, T. Liu, H. Zhao, M. Lan, *Sens. Actuators, B* **2016**, *227*, 583.
- [106] Y. Feng, D. Xiang, Y. Qiu, L. Li, Y. Li, K. Wu, L. Zhu, *Electroanalysis* **2020**, *32*, 571.
- [107] Y. Xue, S. Zheng, H. Xue, H. Pang, *J. Mater. Chem. A* **2019**, *7*, 7301.
- [108] Y. F. Zhang, L. G. Qiu, Y. P. Yuan, Y. J. Zhu, X. Jiang, J. D. Xiao, *Appl. Catal. B* **2014**, *144*, 863.
- [109] J. Yang, H. Ye, Z. Zhang, F. Zhao, B. Zeng, *Sens. Actuators, B* **2017**, *242*, 728.
- [110] F. Xu, B. Jin, H. Li, W. Ju, Z. Wen, Q. Jiang, *New J. Chem.* **2019**, *43*, 18294.
- [111] Y. Luo, Q. Wang, J. Li, F. Xu, L. Sun, Y. Bu, Y. Zou, H. B. Kraatz, F. Rosei, *Inorg. Chem. Front.* **2020**, *7*, 1512.
- [112] X. Xiao, S. Peng, C. Wang, D. Cheng, N. Li, Y. Dong, Q. Li, D. Wei, P. Liu, Z. Xie, D. Qu, X. Li, *J. Electroanal. Chem.* **2019**, *841*, 94.
- [113] V. Archana, Y. Xia, R. Fang, G. Gnana Kumar, *ACS Sustainable Chem.* **2019**, *7*, 6707.
- [114] J. Ding, L. Zhong, X. Wang, L. Chai, Y. Wang, M. Jiang, T. T. Li, Y. Hu, J. Qian, S. Huang, *Sens. Actuators, B* **2020**, *306*, 127551.
- [115] S. eun Kim, A. Muthurasu, *J. Electroanal. Chem.* **2020**, *873*, 114356.
- [116] L. Wang, Y. Xie, C. Wei, X. Lu, X. Li, Y. Song, *Electrochim. Acta* **2015**, *174*, 846.
- [117] L. Zhang, C. Ye, X. Li, Y. Ding, H. Liang, G. Zhao, Y. Wang, *Nano-Micro Lett.* **2018**, *10*, 28.
- [118] Y. Song, C. Wei, J. He, X. Li, X. Lu, L. Wang, *Sens. Actuators, B* **2015**, *220*, 1056.
- [119] Y. Zhang, J. Xu, J. Xia, F. Zhang, Z. Wang, *ACS Appl. Mater. Interfaces* **2018**, *10*, 39151.
- [120] X. Zhang, J. Luo, P. Tang, J. R. Morante, J. Arbiol, C. Xu, Q. Li, J. Fransaeer, *Sens. Actuators, B* **2018**, *254*, 272.
- [121] L. Zhang, Y. Ding, R. Li, C. Ye, G. Zhao, Y. Wang, *J. Mater. Chem. B* **2017**, *5*, 5549.
- [122] G. Mo, X. Zheng, N. Ye, Z. Ruan, *Talanta* **2021**, *225*, 121954.
- [123] J. He, X. Lu, J. Yu, L. Wang, Y. Song, *J. Nanoparticle Res.* **2016**, *18*, 184.
- [124] C. Wei, X. Li, F. Xu, H. Tan, Z. Li, L. Sun, Y. Song, *Anal. Methods* **2014**, *6*, 1550.
- [125] S. Cheng, X. Gao, S. Delacruz, C. Chen, Z. Tang, T. Shi, C. Carraro, R. Maboudian, *J. Mater. Chem. B* **2019**, *7*, 4990.
- [126] Y. Haldorai, S. R. Choe, Y. S. Huh, Y. K. Han, *Carbon* **2018**, *127*, 366.
- [127] I. A. Khan, A. Badshah, M. A. Nadeem, N. Haider, M. A. Nadeem, *Int. J. Hydrogen Energy* **2014**, *39*, 19609.
- [128] H. Zhou, M. Zheng, H. Tang, B. Xu, Y. Tang, H. Pang, *Small* **2020**, *16*, 1904252.
- [129] L. Shi, Y. Li, X. Cai, H. Zhao, M. Lan, *J. Electroanal. Chem.* **2017**, *799*, 512.
- [130] K. Kim, S. Kim, H. N. Lee, Y. M. Park, Y. S. Bae, H. J. Kim, *Appl. Surf. Sci.* **2019**, *479*, 720.
- [131] L. Li, Y. Liu, L. Ai, J. Jiang, *Ind. Eng. Chem. Res.* **2019**, *70*, 330.
- [132] S. A. Abrori, N. L. W. Septiani, Nugraha, I. Anshori, S. Suyatman, V. Suendo, B. Yuliarto, *Sensors* **2020**, *20*, 4891.
- [133] L. Wang, C. Peng, H. Yang, L. Miao, L. Xu, L. Wang, Y. Song, *J. Mater. Sci.* **2019**, *54*, 1654.
- [134] Y. Xie, Y. Song, Y. Zhang, L. Xu, L. Miao, C. Peng, L. Wang, *J. Alloys Compd.* **2018**, *757*, 105.
- [135] P. Arul, S. Abraham John, *J. Electroanal. Chem.* **2017**, *799*, 61.
- [136] L. Hua, Z. Hui, Y. Sun, X. Zhao, H. Xu, Y. Gong, R. Chen, C. Yu, J. Zhou, G. Sun, W. Huang, *Nanoscale* **2018**, *10*, 21006.
- [137] S. Wang, X. Zhang, J. Huang, J. Chen, *Anal. Bioanal. Chem.* **2018**, *410*, 2019.
- [138] E. Asadian, S. Shahrokhian, A. Iraj Zad, *J. Electroanal. Chem.* **2018**, *808*, 114.
- [139] L. Li, B. Zhang, S. Wang, F. Fan, J. Chen, Y. Li, Y. Fu, *Bull. Chem. Soc. Jpn.* **2021**, *94*, 1118.
- [140] A. T. E. Vilian, B. Dinesh, M. Rethinasabapathy, S. K. Hwang, C. S. Jin, Y. S. Huh, Y. K. Han, *J. Mater. Chem. A* **2018**, *6*, 14367.

- [141] Y. Zhang, Y. Zhang, H. Zhu, S. Li, C. Jiang, R. J. Blue, Y. Su, *J. Alloys Compd.* **2019**, *780*, 98.
- [142] A. Muthurasu, H. Y. Kim, *Electroanalysis* **2019**, *31*, 966.
- [143] L. Long, X. Liu, L. Chen, S. Wang, M. Liu, J. Jia, *Electrochim. Acta* **2019**, *308*, 243.
- [144] Y. Zhang, L. Wang, J. Yu, H. Yang, G. Pan, L. Miao, Y. Song, *J. Alloys Compd.* **2017**, *698*, 800.
- [145] J. Chen, H. Yin, J. Zhou, L. Wang, Z. Ji, Y. Zheng, Q. Nie, *Mater. Technol.* **2021**, *36*, 286.
- [146] S. Dong, H. Cui, D. Zhang, M. Tong, *J. Electrochem. Soc.* **2019**, *166*, B193.
- [147] Q. Zhang, L. Zhang, H. Dai, Z. Li, Y. Fu, Y. Li, *J. Electroanal. Chem.* **2018**, *823*, 40.
- [148] Y. Song, M. Xu, C. Gong, Y. Shen, L. Wang, Y. Xie, L. Wang, *J. Mater. Chem. B* **2018**, *257*, 792.
- [149] J. He, H. Yang, Y. Zhang, J. Yu, L. Miao, Y. Song, L. Wang, *Sci. Rep.* **2016**, *6*, 36637.
- [150] Y. Song, Y. Shen, C. Gong, J. Chen, M. Xu, L. Wang, L. Wang, *ChemElectroChem* **2017**, *4*, 1457.
- [151] Z. Kang, K. Jiao, R. Peng, Z. Hu, S. Jiao, *RSC Adv.* **2017**, *7*, 11872.
- [152] M. Shokrehodaei, S. Quinones, *Sensors* **2020**, *20*, 1251.
- [153] H. Xia, N. Li, X. Zhong, Y. Jiang, *Front. Bioeng. Biotechnol.* **2020**, *8*, 695.
- [154] Y. Hu, H. Cheng, X. Zhao, J. Wu, F. Muhammad, S. Lin, J. He, L. Zhou, C. Zhang, Y. Deng, P. Wang, Z. Zhou, S. Nie, H. Wei, *ACS Nano* **2017**, *11*, 5558.
- [155] N. Zhu, L. Gu, J. Wang, X. Li, G. Liang, J. Zhou, Z. Zhang, *J. Phys. Chem. C* **2019**, *123*, 9388.
- [156] M. Y. Shi, M. Xu, Z. Y. Gu, *Anal. Chim. Acta* **2019**, *1079*, 164.
- [157] Z. Zhao, T. Lin, W. Liu, L. Hou, F. Ye, S. Zhao, *Spectrochim. Acta, Part A* **2019**, *219*, 240.
- [158] L. Hang, F. Zhou, D. Men, H. Li, X. Li, H. Zhang, G. Liu, W. Cai, C. Li, Y. Li, *Nano Res.* **2017**, *10*, 2257.
- [159] D. Ning, Q. Liu, Q. Wang, X. M. Du, W. J. Ruan, Y. Li, *Sens. Actuators, B* **2019**, *282*, 443.
- [160] W. Xu, L. Jiao, H. Yan, Y. Wu, L. Chen, W. Gu, D. Du, Y. Lin, C. Zhu, *ACS Appl. Mater. Interfaces* **2019**, *11*, 22096.
- [161] Z. Zhao, J. Pang, W. Liu, T. Lin, F. Ye, S. Zhao, *Microchim. Acta* **2019**, *186*, 295.
- [162] M. Aghayan, A. Mahmoudi, K. Nazari, S. Dehghanpour, S. Sohrabi, M. R. Sazegar, N. Mohammadian-Tabrizi, *J. Porous Mater.* **2019**, *26*, 1507.
- [163] W. Dong, X. Liu, W. Shi, Y. Huang, *RSC Adv.* **2015**, *5*, 17451.
- [164] W. Dong, L. Yang, Y. Huang, *Talanta* **2017**, *167*, 359.
- [165] F. X. Qin, S. Y. Jia, F. F. Wang, S. H. Wu, J. Song, Y. Liu, *Catal. Sci. Technol.* **2013**, *3*, 2761.
- [166] T. Lin, Y. Qin, Y. Huang, R. Yang, L. Hou, F. Ye, S. Zhao, *Chem. Commun.* **2018**, *54*, 1762.
- [167] Y. L. Liu, X. J. Zhao, X. X. Yang, Y. F. Li, *Analyst* **2013**, *138*, 4526.
- [168] F. Cui, Q. Deng, L. Sun, *RSC Adv.* **2015**, *5*, 98215.
- [169] C. Hou, Y. Wang, Q. Ding, L. Jiang, M. Li, W. Zhu, D. Pan, H. Zhu, M. Liu, *Nanoscale* **2015**, *7*, 18770.
- [170] Q. Wang, X. Zhang, L. Huang, Z. Zhang, S. Dong, *Angew. Chem.* **2017**, *56*, 16082.
- [171] X. Yi, W. Dong, X. Zhang, J. Xie, Y. Huang, *Anal. Bioanal. Chem.* **2016**, *408*, 8805.
- [172] G. Zhu, M. Zhang, L. Lu, X. Lou, M. Dong, L. Zhu, *Sens. Actuators, B* **2019**, *288*, 12.
- [173] F. Liu, J. He, M. Zeng, J. Hao, Q. Guo, Y. Song, L. Wang, *J. Nanoparticle Res.* **2016**, *18*, 106.
- [174] B. Tan, H. Zhao, W. Wu, X. Liu, Y. Zhang, X. Quan, *Nanoscale* **2017**, *9*, 18699.
- [175] Y. Huang, M. Zhao, S. Han, Z. Lai, J. Yang, C. Tan, Q. Ma, Q. Lu, J. Chen, X. Zhang, Z. Zhang, B. Li, B. Chen, Y. Zong, H. Zhang, *Adv. Mater.* **2017**, *29*, 1700102.
- [176] Y. Pan, Y. Pang, Y. Shi, W. Zheng, Y. Long, Y. Huang, H. Zheng, *Microchim. Acta* **2019**, *186*, 213.
- [177] P. Du, P. Du, Q. Niu, J. Chen, Y. Chen, J. Zhao, X. Lu, *Anal. Chem.* **2020**, *92*, 7980.
- [178] T. T. Zhao, Z. W. Jiang, S. J. Zhen, C. Z. Huang, Y. F. Li, *Microchim. Acta* **2019**, *186*, 168.
- [179] N. Bagheri, M. Dastborhan, A. Khataee, J. Hassanzadeh, M. Kobya, *Spectrochim. Acta, Part A* **2019**, *213*, 28.
- [180] F. Luo, Y. Lin, L. Zheng, X. Lin, Y. Chi, *ACS Appl. Mater. Interfaces* **2015**, *7*, 11322.
- [181] W. Dong, Y. Zhuang, S. Li, X. Zhang, H. Chai, Y. Huang, *Sens. Actuators, B* **2018**, *255*, 2050.
- [182] Y. Song, D. Cho, S. Venkateswarlu, M. Yoon, *RSC Adv.* **2017**, *7*, 10592.
- [183] X. Qian Tang, Y. Dan Zhang, Z. Wei Jiang, D. Mei Wang, C. Zhi Huang, Y. Fang Li, *Talanta* **2018**, *179*, 43.
- [184] J. W. Zhang, H. T. Zhang, Z. Y. Du, X. Wang, S. H. Yu, H. L. Jiang, *Chem. Commun.* **2014**, *50*, 1092.
- [185] L. Ai, L. Li, C. Zhang, J. Fu, J. Jiang, *Chem. - Eur. J.* **2013**, *19*, 15105.
- [186] A. Kumar, A. R. Chowdhuri, A. Kumari, S. K. Sahu, *Mater. Sci. Eng. C* **2018**, *92*, 913.
- [187] S. Hu, Y. Jiang, Y. Wu, X. Guo, Y. Ying, Y. Wen, H. Yang, *ACS Appl. Mater. Interfaces* **2020**, *12*, 55324.
- [188] P. T. Toi, T. Q. Trung, T. M. L. Dang, C. W. Bae, N. E. Lee, *ACS Appl. Mater. Interfaces* **2019**, *11*, 10707.
- [189] D. K. Sen, G. S. Sarin, *Br. J. Ophthalmol.* **1980**, *64*, 693.
- [190] H. du Toit, R. Rashidi, D. W. Ferdani, M. B. Delgado-Charro, C. M. Sangan, M. Di Lorenzo, *Biosens. Bioelectron.* **2016**, *78*, 411.
- [191] X. Zhu, S. Yuan, Y. Ju, J. Yang, C. Zhao, H. Liu, *Anal. Chem.* **2019**, *91*, 10764.
- [192] X. Xuan, M. Qian, L. Pan, T. Lu, L. Han, H. Yu, L. Wan, Y. Niu, S. Gong, *J. Mater. Chem. B* **2020**, *8*, 9094.
- [193] Z. Wei, W. Zhu, Y. Li, Y. Ma, J. Wang, N. Hu, Y. Suo, J. Wang, *Inorg. Chem.* **2018**, *57*, 8422.
- [194] L. Hou, H. Zhao, S. Bi, Y. Xu, Y. Lu, *Electrochim. Acta* **2017**, *248*, 281.
- [195] X. Wei, J. Guo, H. Lian, X. Sun, B. Liu, *Sens. Actuators, B* **2020**, *329*, 129205.
- [196] Z. Zhao, Y. Kong, X. Lin, C. Liu, J. Liu, Y. He, L. Yang, G. Huang, Y. Mei, *J. Mater. Chem. A* **2020**, *8*, 26119.
- [197] Z. Wang, T. Liu, L. Jiang, M. Asif, X. Qiu, Y. Yu, F. Xiao, H. Liu, *ACS Appl. Mater. Interfaces* **2019**, *11*, 32310.
- [198] C. Chen, Y. Zhong, S. Cheng, Y. Huang, T. Li, T. Shi, G. Liao, Z. Tang, *J. Electrochem. Soc.* **2020**, *167*, 027531.
- [199] X. Li, Q. Feng, K. Lu, J. Huang, Y. Zhang, Y. Hou, H. Qiao, D. Li, Q. Wei, *Biosens. Bioelectron.* **2021**, *171*, 112690.
- [200] W. Ling, G. Liew, Y. Li, Y. Hao, H. Pan, H. Wang, B. Ning, H. Xu, X. Huang, *Adv. Mater.* **2018**, *30*, 1800917.
- [201] D. S. A Paul, A. Jibinlal, *Sens. Trans. J.* **2018**, *11*, 20.
- [202] P. H. Huang, C. P. Hong, J. F. Zhu, T. T. Chen, C. T. Chan, Y. C. Ko, T. L. Lin, Z. B. Pan, N. K. Sun, Y. C. Wang, J. J. Luo, T. C. Lin, C. C. Kang, J. J. Shyue, M. L. Ho, *Dalton Trans.* **2017**, *46*, 6985.
- [203] H. Cheng, L. Zhang, J. He, W. Guo, Z. Zhou, X. Zhang, S. Nie, H. Wei, *Anal. Chem.* **2016**, *88*, 5489.
- [204] C. A. Vu, W. Y. Chen, *Sensors* **2019**, *19*, 4214.
- [205] A. Matsumoto, Y. Miyahara, *Nanoscale* **2013**, *5*, 10702.
- [206] G. Seo, G. Lee, M. J. Kim, S. H. Baek, M. Choi, K. B. Ku, C. S. Lee, S. Jun, D. Park, H. G. Kim, S. J. Kim, J. O. Lee, B. T. Kim, E. C. Park, S. Il Kim, *ACS Nano* **2020**, *14*, 5135.
- [207] Y. H. Kwak, D. S. Choi, Y. N. Kim, H. Kim, D. H. Yoon, S. S. Ahn, J. W. Yang, W. S. Yang, S. Seo, *Biosens. Bioelectron.* **2012**, *37*, 82.
- [208] B. Veigas, E. Fortunato, P. V. Baptista, *Sensors* **2015**, *15*, 10380.
- [209] B. Wang, Y. Luo, B. Liu, G. Duan, *ACS Appl. Mater. Interfaces* **2019**, *11*, 35935.

- [210] B. Wang, Y. Luo, L. Gao, B. Liu, G. Duan, *Biosens. Bioelectron.* **2021**, 171, 112736.
- [211] C. Xiong, L. Tian, C. Xiao, Z. Xue, F. Zhou, H. Zhou, Y. Zhao, M. Chen, Q. Wang, Y. Qu, Y. Hu, W. Wang, Y. Zhang, X. Zhou, Z. Wang, P. Yin, Y. Mao, Z. Q. Yu, Y. Cao, X. Duan, L. Zheng, Y. Wu, *Sci. Bull.* **2020**, 65, 2100.
- [212] C. Xiong, T. Zhang, W. Kong, Z. Zhang, H. Qu, W. Chen, Y. Wang, L. Luo, L. Zheng, *Biosens. Bioelectron.* **2018**, 101, 21.
- [213] G. M. Whitesides, *Nature* **2006**, 442, 368.
- [214] S. K. Sia, G. M. Whitesides, *Electrophoresis* **2003**, 24, 3563.
- [215] J. W. Hong, V. Studer, G. Hang, W. F. Anderson, S. R. Quake, *Nat. Biotechnol.* **2004**, 22, 435.
- [216] R. Gómez-Sjöberg, A. A. Leyrat, D. M. Pirone, C. S. Chen, S. R. Quake, *Anal. Chem.* **2007**, 79, 8557.
- [217] J. F. Zhong, Y. Chen, J. S. Marcus, A. Scherer, S. R. Quake, C. R. Taylor, L. P. Weiner, *Lab. Chip* **2007**, 8, 68.
- [218] T. Vilkner, D. Janasek, A. Manz, *Anal. Chem.* **2004**, 76, 3373.
- [219] E. Delamarche, D. Juncker, H. Schmid, *Adv. Mater.* **2005**, 17, 2911.
- [220] K. Jähnisch, V. Hessel, H. Löwe, M. Baerns, *Angew. Chem., Int. Ed.* **2004**, 43, 406.
- [221] A. De Mello, R. Wootton, *Lab Chip* **2002**, 2, 7N.
- [222] Y. Kikutani, T. Kitamori, *Macromol. Rapid Commun.* **2004**, 25, 158.
- [223] C. C. Lee, G. Sui, A. Elizarov, C. J. Shu, Y. S. Shin, A. N. Dooley, J. Huang, A. Daridon, P. Wyatt, D. Stout, H. C. Kolb, O. N. Witte, N. Satyamurthy, J. R. Heath, M. E. Phelps, S. R. Quake, H. R. Tseng, *Science* **2005**, 310, 1793.
- [224] J. Wang, G. Sui, V. P. Mocharla, R. J. Lin, M. E. Phelps, H. C. Kolb, H. R. Tseng, *Angew. Chem., Int. Ed.* **2006**, 45, 5276.
- [225] B. J. Kirby, T. J. Shepodd, E. F. Hasselbrink, *J. Chromatogr. A* **2002**, 979, 147.
- [226] M. A. Unger, H. P. Chou, T. Thorsen, A. Scherer, S. R. Quake, *Science* **2000**, 288, 113.
- [227] A. D. Stroock, S. K. W. Dertinger, A. Ajdari, I. Mezić, H. A. Stone, G. M. Whitesides, *Science* **2002**, 295, 647.
- [228] W. Gu, X. Zhu, N. Futai, B. S. Cho, S. Takayama, *Proc. Natl. Acad. Sci. USA* **2004**, 101, 15861.
- [229] H. Hartanto, M. Wu, M. L. Lam, T. H. Chen, *Biomicrofluidics* **2020**, 14, 061507.
- [230] J. Reboud, G. Xu, A. Garrett, M. Adriko, Z. Yang, E. M. Tukahebwa, C. Rowell, J. M. Cooper, *Proc. Natl. Acad. Sci. USA* **2019**, 116, 4834.
- [231] C. S. Karamitros, M. Morvan, A. Vigne, J. Lim, P. Gruner, T. Beneyton, J. Vrignon, J. C. Baret, *Anal. Chem.* **2020**, 92, 4908.
- [232] M. G. Pollack, A. D. Shenderov, R. B. Fair, *Lab Chip* **2002**, 2, 96.
- [233] Y. Song, B. Lin, T. Tian, X. Xu, W. Wang, Q. Ruan, J. Guo, Z. Zhu, C. Yang, *Anal. Chem.* **2019**, 91, 388.
- [234] I. Ortiz-Gómez, A. Salinas-Castillo, A. G. García, J. A. Álvarez-Bermejo, I. de Orbe-Payá, A. Rodríguez-Diéguez, L. F. Capitán-Vallvey, *Microchim. Acta* **2018**, 185, 47.
- [235] M. Mohammad, A. Razmjou, K. Liang, M. Asadnia, V. Chen, *ACS Appl. Mater. Interfaces* **2019**, 11, 1807.
- [236] H. Li, M. Eddaoudi, M. O'Keeffe, O. M. Yaghi, *Nature* **1999**, 402, 276.



Muhammed Adeel is a third year Ph.D. student with Prof Flavio Rizzolio and Prof Vincenzo Canzonieri, in Science and Technology of Bio and Nanomaterials at the University Cà Foscari of Venice (Italy). His current research activity focuses on nonenzymatic electrochemical glucose sensors, using 2D metal organic frameworks (MOFs), and on the development of new materials for applications in cancer therapy.



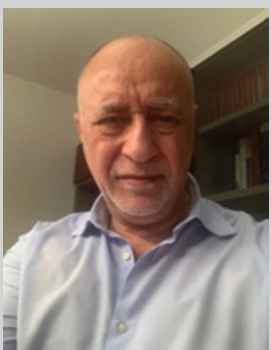
Kanwal Asif is a second year Ph.D. student with Prof Flavio Rizzolio, and Prof Vincenzo Canzonieri in Science and Technology of Bio and Nanomaterials at the University Cà Foscari of Venice (Italy). Her current research activity focuses on the use of self-therapeutic nanomaterials for cancer therapy.



Md. Mahbubur Rahman has been an assistant professor at Konkuk University, South Korea, since 2014. He received an M.S. degree in Inorganic & Analytical Chemistry in 2005 from the University of Dhaka, Bangladesh, and a Ph.D. degree in electrochemistry in 2014 from Konkuk University. He also worked as a postdoctoral scholar at Incheon National University. His research interests include the development of nanomaterials for various electrochemical and photo-electrochemical technologies such as sensors/biosensors, solar cells, and energy storage devices.



Salvatore Daniele is full professor of Analytical Chemistry at the Department of Molecular Science and Nanosystems at the University Cà Foscari Venice (Italy). He is member of the International Society of Electrochemistry (ISE), and in the past was appointed as Chair of the Division 1 (Analytical Electrochemistry). His research activity focuses on the development of electrochemical sensors for electroanalysis in synthetic and real samples, including food and biologic fluids, and on investigation of electrode processes using micro/nanoelectrodes and scanning electrochemical microscopy.



Vincenzo Canzonieri is currently associate professor of Pathology at the University of Trieste and Director of the Pathology Department at the Aviano Cancer Center CRO, NCI. He attended the Residency in Anatomic Pathology at the University of Padova, the Residency in General Oncology at the University of Catania and the residency in Forensic Medicine at the University of Udine. He obtained also a mini MBA in sanitary management at the University Bocconi in Milan in 2010. His research activities focus on digital pathology and morphological, phenotypic and genotypic characterizations of GYN, GI, soft tissue tumors and lymphomas.



Flavio Rizzolio is full professor in Molecular Biology at the Department of Molecular Science and Nanosystems at the University Cà Foscari of Venice (Italy). His work started by studying the genetic alterations causative of ovarian dysfunctions, followed by a second phase dedicated to the mechanisms of cell cycle control in cancer and finally, a nanomedicine approach for cancer therapy.